



PpT measurements of Glycols (Mono-, Di- and Triethylene glycol) up to 423.15 K and 140.0 MPa and their aqueous solutions at atmospheric pressure

Trancoso, Julia; Kontogeorgis, Georgios M.; Liang, Xiaodong; von Solms, Nicolas

Published in:
Fluid Phase Equilibria

Link to article, DOI:
[10.1016/j.fluid.2023.113980](https://doi.org/10.1016/j.fluid.2023.113980)

Publication date:
2024

Document Version
Publisher's PDF, also known as Version of record

[Link back to DTU Orbit](#)

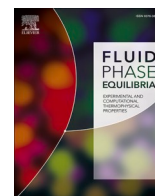
Citation (APA):
Trancoso, J., Kontogeorgis, G. M., Liang, X., & von Solms, N. (2024). PpT measurements of Glycols (Mono-, Di- and Triethylene glycol) up to 423.15 K and 140.0 MPa and their aqueous solutions at atmospheric pressure. *Fluid Phase Equilibria*, 577, Article 113980. <https://doi.org/10.1016/j.fluid.2023.113980>

General rights

Copyright and moral rights for the publications made accessible in the public portal are retained by the authors and/or other copyright owners and it is a condition of accessing publications that users recognise and abide by the legal requirements associated with these rights.

- Users may download and print one copy of any publication from the public portal for the purpose of private study or research.
- You may not further distribute the material or use it for any profit-making activity or commercial gain
- You may freely distribute the URL identifying the publication in the public portal

If you believe that this document breaches copyright please contact us providing details, and we will remove access to the work immediately and investigate your claim.



P ρ T measurements of Glycols (Mono-, Di- and Triethylene glycol) up to 423.15 K and 140.0 MPa and their aqueous solutions at atmospheric pressure

Julia Trancoso, Georgios M. Kontogeorgis, Xiaodong Liang, Nicolas von Solms*

Center for Energy Resources Engineering (CERE), Department of Chemical and Biochemical Engineering, Technical University of Denmark (DTU), Kongens Lyngby 2800, Denmark

ARTICLE INFO

Keywords:

Glycol
Density
Experimental measurements
Cubic-plus-association
PC-SAFT

ABSTRACT

The density of three glycols, namely Monoethylene glycol (MEG), Diethylene glycol (DEG), and Triethylene glycol (TEG) was measured in the temperature range from 298.15 K to 423.15 K and pressures up to 140.0 MPa using a vibrating tube density meter Anton Paar DMA-HPM, coupled with a high-pressure mPDS 5 unit. The modified Tait-Tammann equation was used to correlate the experimental density, which gave an absolute average relative deviation (AARD) of less than 0.2 %. Derived properties such as isobaric thermal expansion and isothermal compressibility coefficients were estimated and discussed. Furthermore, the density of the binary systems composed by the aforementioned glycols (1) + water (2) was also measured in the (273.15, 373.15) K temperature range at atmospheric pressure. The Cubic-Plus-Association (CPA) and the simplified version of the Perturbed-Chain Statistical Associating Fluid Theory (PC-SAFT) equations of state were used to correlate the newly measured data, with deviations less than 3.7 % for pure component and 12.0 % for the binary systems.

1. Introduction

Monoethylene glycol (MEG), diethylene glycol (DEG), and triethylene glycol (TEG) are the first members of a homologous series of diols commonly used as reactants and intermediates in a variety of industrial applications. MEG is used primarily as an antifreeze in motor vehicles, water heating systems, solar energy systems, heat pumps, and industrial cooling systems. Approximately 40.0 % of total monoethylene glycol production goes into the manufacture of polyester fibers. It is also used to a lesser extent as a humectant, plasticizer, softener, hydraulic fluid. DEG is commonly used as a solvent, softener in paper, adhesives, and cork industries, deicing agent for runways and aircraft, and as a dye additive in printing and stamping inks. TEG is used in air conditioning systems as a dehumidifier, as a vinyl plasticizer, or as an intermediate in the production of polyols and resins [1]. In the oil and gas industry, MEG is an important hydrate inhibitor, while both DEG and TEG are used as dehydrating agents in natural gas processing [2,3]. Process design for such applications relies on process simulators that use thermodynamic data, which, in turn, are parameterized using consistent thermophysical data. In the case of glycols, however, these properties are not fully and accurately characterized, being new P ρ T data of great importance for the

development of new technologies and the improvement/optimization of existing processes.

Beyond the practical viewpoint, glycols also provide an interesting theoretical study because they present a unique two adjacent hydroxyl groups, that give rise to strong self-associated fluids [4], and intramolecular hydrogen bonding [5–7]. In this context, the P ρ T behavior provides a good analysis of these intermolecular forces, since the hydrogen bonds change with pressure. Lafitte et al. [8] have emphasized that, although the optimal EoS parameterization is still under debate, the simultaneous description of the density and its pressure and temperature derivatives appear to be the most relevant properties to consider [9] in order to achieve a realistic balance between dispersive and associative energies. In this context, aiming to extend the accurate thermophysical characterization of glycols, the density as a function of pressure (up to 140.0 MPa) and temperature (298.15, 423.15) K was investigated for the first three members of the glycol series: Mono-(MEG), Di- (DEG), and Triethylene (TEG) glycol. The modified Tait-Tammann equation was used to correlate the experimental data, and the derived properties, such as isobaric thermal expansion coefficients and isothermal compressibility, were estimated. The density of the binary systems composed by the aforementioned glycols (1) + water

* Corresponding author.

E-mail address: nvs@kt.dtu.dk (N. von Solms).

<https://doi.org/10.1016/j.fluid.2023.113980>

Received 18 August 2023; Received in revised form 12 October 2023; Accepted 17 October 2023

Available online 18 October 2023

0378-3812/© 2023 The Author(s). Published by Elsevier B.V. This is an open access article under the CC BY license (<http://creativecommons.org/licenses/by/4.0/>).

Table 1
Literature review of density measurements under pressure for pure MEG, DEG, TEG.

Compound	T _{range} (K)	P _{range} (MPa)	N _{points}	Year	Refs.
MEG	273.15–368.15	0.1–1176.8	36	1932	Bridgman [14]
MEG	298.20–348.20	0.1–6.9	21	1990	Wong [15]
MEG	298.15	50.0–200.0	4	1990	Miyamoto [16]
MEG	288.13	0.1–349.4	24	2010	Guignon [17]
MEG	278.15–333.15	0.1–100.0	35	2010,2011,2013	Egorov [18–20]
MEG	278.15–358.15	0.1–60.0	126	2013	Atilhan [21] ¹
MEG	293.14–393.09	4.8–100.0	89	2020	Yang [22]
MEG	293.15–413.15	0.1–60.0	154	2022	Zaric [23]
DEG	323.14–498.11	Saturation Line	8	2002	Steele [24]
TEG	313.14–473.11	Saturation Line	7	2002	Steele [25]
DEG, TEG	293.15–363.15	0.1–70.0	160	2019	Pereira [28]
MEG, DEG, TEG	293.15–464.60	0.1–245.2	148	2012	Sagdeev [26] ¹
MEG, DEG, TEG	283.08–363.18	0.1–95.0	216	2017	Crespo [27]

Table 2
Literature review of density measurements of glycol (1) + water (2) at atmospheric pressure.

Compound (1)	T _{range} (K)	N _{points}	Year	Ref.
MEG	298.15	14	1971	Hayduk ^[29]
MEG	303.15	15	1982	Dizechi ^[30]
MEG	283.15–303.15	87	1990	Lee ^[34]
MEG	308.15	11	1994	Reddy ^[31]
MEG	283.15–313.15	52	1998	Tsierkezos ^[35]
MEG	293.15–353.15	77	2003	Yang ^[36]
MEG	308.15–323.15	52	2008	Zhang ^[37]
MEG	288.15–303.15	133	2016	Moosavi ^[38]
DEG	283.15–353.15	195	2008	Garcia ^[39]
DEG	303.15–323.15	85	2011	Begum ^[40]
DEG	278.15–333.15	252	2016	Klimaszewski ^[41]
TEG	303.15–323.15	80	2013	Begum ^[42]
TEG	078.15–333.15	372	2015	Klimaszewski ^[43]
MEG, DEG	298.15	22	1995	Aminabhavi ^[32]
MEG, DEG, TEG	288.15–308.15	58	1978	Moréni ^[44]
MEG, DEG, TEG	298.15–323.15	132	1991	Müller ^[45]
MEG, DEG, TEG	293.85–445.85	84	2003	Sun ^[33]

Table 3
List of compounds used in this work and their purities.

Chemical Name	Acronym	Provider	Purity ^a
Decane	C ₁₀ H ₂₂	Sigma Aldrich	≥ 95 %
Water	H ₂ O	Elix Reference 5	≥ 99 %
Monoethylene glycol	MEG	Sigma Aldrich	≥ 99 %
Diethylene glycol	DEG	Fluka	≥ 99 %
Triethylene glycol	TEG	Fluka	≥ 99 %

^a As determined by gas chromatography (GC) by the supplier.

^b Conductivity at 298.15 K: 10–15 μS/cm.

(2) was also measured in the (273.15, 373.15) K temperature range at atmospheric pressure. In addition, the Cubic-Plus-Association (CPA) and a simplified version of the Perturbed-Chain Statistical Associating Fluid Theory (PC-SAFT) EoS were proposed to model the reported experimental data and contribute to the current discussion on the performance of these models over wide temperature and pressure ranges [10,11].

2. Literature review

Although glycols density data at or near atmospheric pressure is widely available in the literature (see Carvalho et al. [12] for a complete review of 11 glycols and glymes or Sagdeev et al. [13] for a review focused on MEG, DEG and TEG), PpT data are scarcer. For MEG, 12 density data are available under pressure, being the most studied compound in the series. Bridgman [14] was the first one to report MEG densities at high pressures (up to 1176.8 MPa) along three isotherms of

273.15 K, 323.15 K, and 368.15 K by using Bellows volumetric indirect measurements. Wong and Hayduk [15] obtained directly data by using an Anton Paar densitometer equipped with a high-pressure cell in the very restricted pressure range (up to 6.9 MPa) and temperatures between (298.20, 348.20) K. In the same year, Miyamoto et al. [16] extended the isotherm of 298.15 K up to 200.0 MPa, while some year later Guignon et al. [17] extended the single 288.13 K isotherm up to 349.4 MPa with a variable volume piezometer with a solid-piston volumeter. The compressibility data reported in a series of studies by Egorov et al. [18–20] covered the temperature (278.15, 333.15) K and pressure (0.1, 100.0) MPa ranges. Measurements were performed using constant volume piezometer. Atilhan et al. [21] also measured densities in a more wide range of temperatures (278.15, 358.15) K and pressures (up to 60.0 MPa). Their study is also the first one to apply a thermodynamic model (PC-SAFT) for experimental data correlation. More recently, Yang et al. [22] and Zaric et al. [23] work extended the current data situation for MEG density, investigating it over the temperature (283.15, 393.09) K and pressure (4.8, 100.1) MPa ranges for the first and (293.15, 413.15) K, (0.1, 60.0) MPa for the second group. Both studies used a high-pressure vibrating-tube densimeter.

Fewer data are available for the other two glycols. Steele et al. [24, 25] reported saturated liquid densities for DEG and TEG, covering the (323.14, 498.11) K temperature range for DEG and (313.14, 473.11) K for TEG. At these temperature ranges, the values of vapor pressure for these systems are within 0.002–0.168 MPa. Sagdeev et al. [26] considerably extended the temperature and pressure ranges of the previous studies and provided new accurately density and viscosity data for MEG, DEG, TEG and their mixtures at high temperatures (293.15, 464.60) K and high pressures (up to 245.2 MPa). Thereafter, Crespo et al. [27] published new experimental density data of six glycols, (MEG, DEG, TEG, tetraethylene glycol (TeEG), pentaethylene glycol (PeEG), hexaethylene glycol (HeEG), and a polyethyleneglycol (PEG 400) in a wide range of temperatures (283.08, 363.18) K and pressures (0.1, 95.0) MPa. The study is completed with the modeling of the experimental data using the soft-SAFT equation of state. More recently, Pereira et al. [28] work presents new density measurements of compressed liquid DEG, TEG, and TeEG have been performed using an Anton Paar vibrating U-tube densimeter, in a range of temperatures from about (293.15, 363.15) K and at pressures up to about 70.0 MPa. Table 1 summarizes the density experimental data discussed above.

A similar situation is found for binary systems. The literature survey reveals that although volumetric data on glycol + water systems are available, most of them are very limited. For MEG aqueous solutions, for example, works are concentrated only on one isotherm [29–32] or on a very narrow temperature range of (283.15, 313.15) K. Fewer articles are devoted to mixtures of water and di-, and triethylene glycol, and only between (278.15, 333.15) K. Although Sun et al. [33] have presented a wide temperature range study (293.85, 445.85) K, the results are only for three mixture compositions (x₁ = 0.25, 0.5, and 0.75). In addition, many of these studies used a pycnometer technique for the

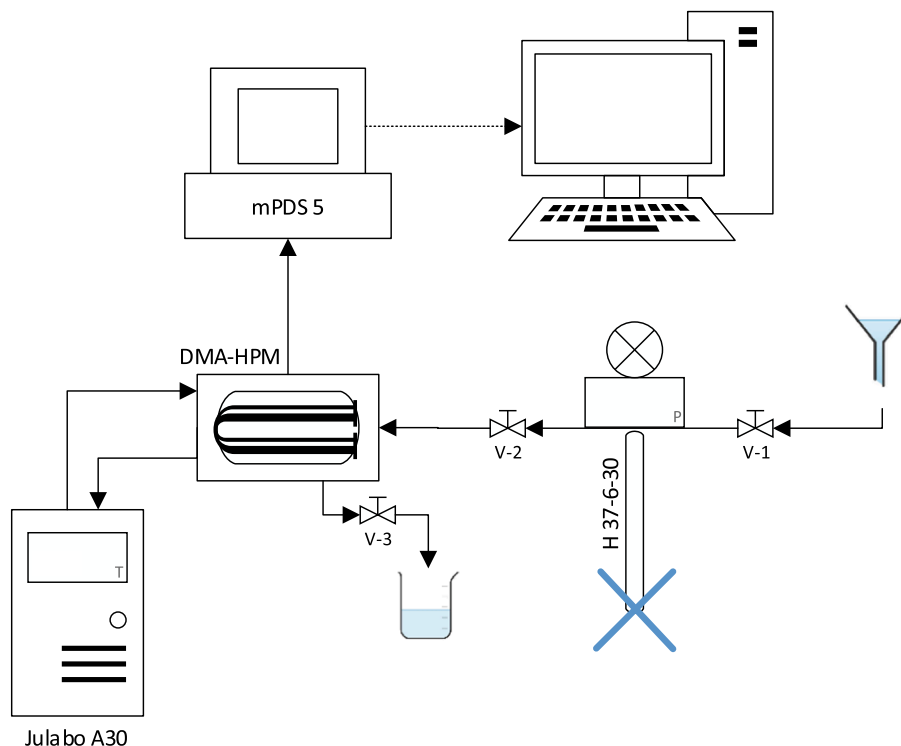


Fig. 1. Schematic representation of the experimental setup used for high-pressure density measurements.

measurements, which does not provide sufficiently accurate results to determine the value of the partial molar volume of the mixture. The data discussed above are shown in Table 2.

3. Materials and methods

3.1. Materials

The compounds used in this work along with their purity are presented in Table 3. These chemicals were used without further purification. All liquids were degassed at ambient conditions for 3600 s by means of an ultrasonic bath Branson 1510 DTH prior to their use.

3.2. Pure component methodology

Densities for the three pure glycols were measured in the (298.15 to 423.15) K temperature and (0.1 to 140.0) MPa pressure ranges using a vibrating tube density meter Anton Paar DMA-HPM, coupled with a mPDS 5 unit. Density was deduced from the resonant frequency of the U-shaped tube containing the fluid, as the oscillation periods are displayed with seven significant figures. The equipment was connected to a pressure line comprising a manual pressure generator (HiP 37–6–30) and a pressure transducer SIKA type P, which measures the pressure up to 150.0 MPa with a 0.05 % FS uncertainty. The measuring cell was thermostated by a circulating liquid bath Julabo PRESTO A30. The temperature was measured by means of a Pt100 inserted inside the cell with an uncertainty of ± 0.02 K. A schematic of the experimental setup is presented in Fig. 1.

After temperature established at the desired value, the degassed sample was loaded in a glass funnel connected to the equipment. Thereafter, the manual pressure generator (HiP 37–6–30) was completely fulfilled with the sample, keeping V-2 closed and V-1 open. The manual valve was then pressed until about 3 ml of the sample was purged through V-2 and V-3, while V-1 was kept closed. This procedure removes any contaminant present in the line, while also ensuring that the entire equipment is filled with the desired sample, removing

bubbles. After that, V-3 was closed, and the manual valve was used to achieve the desired pressure.

Temperature and period data are recorded using an Excel tool provided by Anton Paar. For every temperature and pressure condition, stability is considered to be achieved when the standard deviation of the last 30 recorded values is lower than 0.02 K in temperature and $5 \cdot 10^{-3}$ μ s in oscillation period. It is well known that for viscosities lower than 100 mPa.s the viscosity has little to no impact on the density determination, making the density correction unnecessary. In this work the expanded ($k = 2$) uncertainty of the density measurements is considered to be $7 \cdot 10^{-4}$ $\text{g} \cdot \text{cm}^{-3}$ for $T < 373.15$ K, $5 \cdot 10^{-3}$ $\text{g} \cdot \text{cm}^{-3}$ for $T \geq 373.15$ K at 0.1 MPa, and $3 \cdot 10^{-3}$ $\text{g} \cdot \text{cm}^{-3}$ for $TT \geq 373.15$ K and higher pressures, as concluded by Segovia et al. [46].

The calibration of the density meter was performed using as reference fluids vacuum, Milli-Q water, and decane, in an analogous way to that described by Comuñas et al. [47]. The same methodology has already been used several times in previous works with our equipment [48–50].

The equations used to obtain the density values from the measured oscillation periods are as follows:

For $T < 373.15$ K and $P = 0.1$ MPa:

$$\rho(T, P) = \rho_w(T, P) + \rho_w(T, 0.1 \text{ MPa}) \frac{\tau^2(T, P) - \tau_{\text{water}}^2(T, P)}{\tau_{\text{water}}^2(T, 0.1 \text{ MPa}) - \tau_{\text{vacuum}}^2(T)} \quad (1)$$

For $T > 373.15$ K and $P = 0.1$ MPa:

$$\rho(T, P) = \rho_d(T, P) + \rho_d(T, 0.1 \text{ MPa}) \frac{\tau^2(T, P) - \tau_{\text{decane}}^2(T, P)}{\tau_{\text{decane}}^2(T, 0.1 \text{ MPa}) - \tau_{\text{vacuum}}^2(T)} \quad (2)$$

For any other conditions, i.e., $T > 373.15$ K and $P > 0.1$ MPa:

$$\rho(T, P) = \rho_w(T, P) + \rho_d(T, 0.1 \text{ MPa}) \frac{\tau^2(T, P) - \tau_{\text{water}}^2(T, P)}{\tau_{\text{decane}}^2(T, 0.1 \text{ MPa}) - \tau_{\text{vacuum}}^2(T)} \quad (3)$$

Where T is temperature, P is pressure, τ is the oscillation period, and ρ is density.

Table 4
CPA pure component parameters used in this work.

Compound	b (cm ³ .mol ⁻¹)	$\Gamma = \frac{a_0}{R}$ (K)	c ₁	$\beta \cdot 10^3$	$\frac{\epsilon}{R}$ (K)	Association Scheme	Refs.
MEG	51.40	2531.71	0.6744	14.10	2375.75	4C	[55]
	49.94	2541.44	0.6520	14.53	2384.90	4C	
	49.81	2180.88	1.0550	17.55	2603.50	3C	[56]
	50.18	2296.56	0.8840	12.72	2224.40	4E	
DEG	50.08	2405.18	0.8090	11.96	2347.40	4F	
	92.10	3448.78	0.7991	6.40	2367.57	4C	[55]
	132.10	3562.48	1.1692	18.80	1724.44	4C	[55]
TEG	129.10	3153.10	1.3486	16.62	1438.80	5C	
	128.41	3186.50	1.3567	22.77	1592.70	4F	
	128.57	3122.20	1.3813	20.99	1478.80	5F	[57]
	128.95	3144.40	1.3576	16.62	1451.60	6F	
Water	14.515	1071.34	0.6736	69.20	2003.25	4C	[58]

3.3. Binary systems methodology

For the aqueous solutions of glycols, densities were measured using a DMA 4500 M Anton Paar density meter, which uses the pulsed excitation method. This equipment requires samples of approximately 1 ml, and has measuring time of 30 s, with an accuracy of 0.000005 g.cm³ on density and 0.02 K on temperature. Densities for the aqueous solutions of glycols were measured in the (273.15 to 373.15) K temperature range and atmospheric pressure. The expanded ($k = 2$) uncertainty of the density measurements is calculated as 8.10⁻³ g.cm⁻³.

3.4. Thermodynamic modeling

3.4.1. The cubic-plus-association (CPA)

The Cubic-Plus-Association (CPA) equation of state (EoS) (Eq. (4)) was developed with the purpose of combining the simplicity of the cubic Soave-Redlich-Kwong (SRK) EoS with the association term derived from Wertheim's first-order thermodynamic perturbation theory (TPT-1) to account for specific site-site interactions [51].

$$P = \frac{RT}{V_m - b} - \frac{a(T)}{V_m(V_m + b)} - \frac{RT}{2V_m} \left(1 + \frac{1}{V_m} \frac{\partial \ln g}{\partial \left(\frac{1}{V_m} \right)} \right) \sum_i x_i \sum_{A_i} (1 - X_{A_i}) \quad (4)$$

In Eq. (4) the first two terms are the classical SRK repulsive and attractive components, where P , T , V_m , and R are the pressure, temperature, molar volume, and the universal gas constant, respectively. In the last term, the association contribution is presented in the form derived by Michelsen and Hendriks [52]. This expression is mathematically identical to the original one proposed by Chapman et al. [53] but simpler, simplifying and speeding-up the calculations, in particular, when derivatives are needed. Here, X_{A_i} is the fraction of A-sites on molecule i that do not form bonds with other active sites and satisfies the following equation (Eq. (5)):

$$X_{A_i} = \frac{1}{1 + \frac{1}{V_m} \sum_j x_j \sum_{B_j} (X_{B_j} \Delta^{A_i B_j})} \quad (5)$$

Where $\Delta^{A_i B_j}$, the association strength between site A on molecule i and site B on molecule j is given by Eq. (6):

$$\Delta^{A_i B_j} = g(V_m) \left[\exp \left(\frac{\epsilon^{A_i B_j}}{RT} \right) - 1 \right] b_{ij} \beta^{A_i B_j} \quad (6)$$

$\epsilon^{A_i B_j}$ and $\beta^{A_i B_j}$ are the association energy and volume of interaction, respectively, and $g(V_m)$ is the radial distribution function for the reference fluid. In this work, all phase equilibria calculations were performed using the 1999 simplified CPA version [54] which employs the simplified radial distribution function (Eq. (7)).

$$g(V_m) = \frac{1}{1 - 1.9\eta} \quad \text{where } \eta = \frac{1}{4V_m} b \quad (7)$$

In total, CPA has five pure-compound parameters. Three of them are used directly in the SRK terms in Eq. (4), being b the co-volume of the compound, and a_0 and c_1 implemented inside the a -function (Eq. (8)), which also depends on the temperature ($T_R = T/T_c$).

$$a(T) = a_0 \left(1 + c_1 \left(1 - \sqrt{T_R} \right) \right)^2 \quad (8)$$

Meanwhile, two additional parameters for associating compounds ($\epsilon^{A_i B_j}$, $\beta^{A_i B_j}$) are required to describe the association contribution. As seen in Eq. (5) and Table 4, another important element in the CPA association term is the choice of the association scheme. The CPA pure component parameters and a schematic representation of the different association schemes used in this work are shown in Table 4 and Table 5, respectively.

When extending the model to mixtures, the pure component parameters are subject to combining and mixing rules. In this work, the CR-1 rule has been applied for the association parameters, where the association energy is obtained by the arithmetic average, and a geometric average is used for the association volume. For the SRK parameters, the standard the van der Waals one-fluid (vdW1) mixing rules Eqs. (9)–(11) have been applied:

$$a(T)_{\text{mix}} = \sum_i \sum_j x_i x_j a_{ij}(T) \quad (9)$$

$$b_{\text{mix}} = \sum_i x_i b_i \quad (10)$$

Where:

$$a_{ij}(T) = \sqrt{a_i(T) \cdot a_j(T)} (1 - k_{ij}) \quad (11)$$

Where k_{ij} is the binary interaction parameter (BIP).

CPA has been shown to provide good predictive ($k_{ij} = 0$) results for mixtures of natural gas and water, giving comparable performance to the empirical GERG-water correlation [60]. However, as shown in literature [61–63] with the incorporation of another associating compound as glycols this BIP is required. Table 6 summarizes the binary interaction parameter used in this work within the CPA framework:

3.4.2. The perturbed-chain statistical associating fluid theory (PC-SAFT)

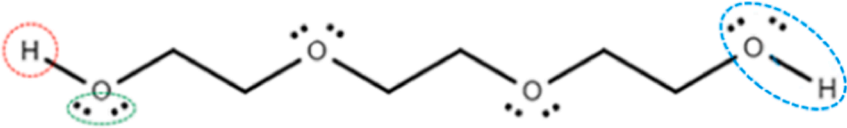
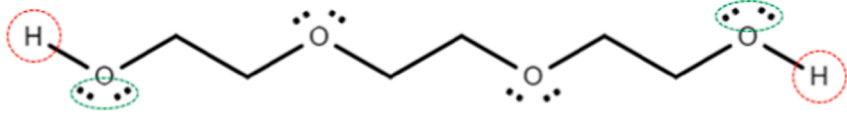
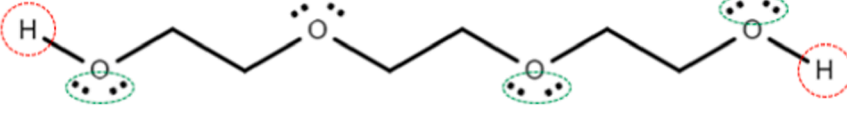
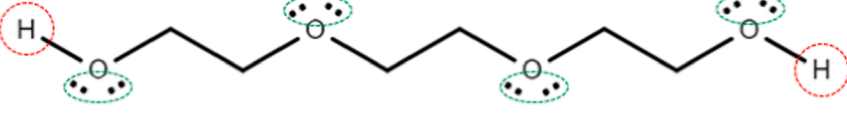
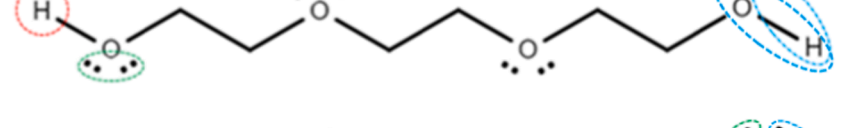
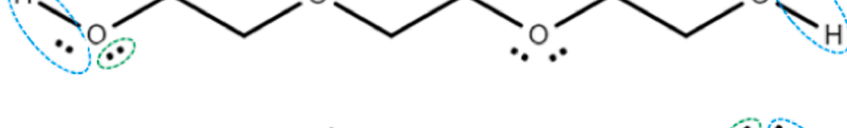
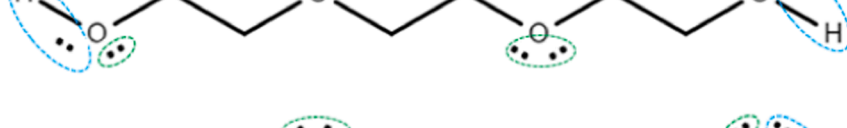


The PC-SAFT EoS was developed by Gross and Sadowski [65], in which the reduced residual Helmholtz free energy for mixtures containing non-associating fluids in PC-SAFT is given by

$$a^r = a^{\text{hs}} + a^{\text{chain}} + a^{\text{disp}} \quad (12)$$

Where a^{hs} and a^{chain} are the contributions from hard-sphere segment–segment interactions and chain formation, respectively. The sum

Table 5

Association schemes used in this work within the CPA framework originally based on and extended from Huang and Radosz [59] terminology. Red represents positive, green negative, and blue bipolar sites. A bipolar site is able to associate with both positive and negative sites.

Compound	Representation	Association Type
Glycol		3C
		4C
		5C
		6D
		4E
		4F
		5F
		6F
Water		4C

of these last two is the reference to build the dispersion contribution a^{disp} . The simplified version of PC-SAFT proposed by von Solms et al. [66] was used in this work, where non-associating molecules are characterized by three pure component parameters: the chain length (m_{chain}), the segment diameter (σ), and the segment energy (ϵ). The conventional Berthelot–Lorentz combining rules were employed for σ_{ij} and ϵ_{ij} Eqs. (13) and

((14)) and the binary interaction parameter k_{ij} is introduced to correct the dispersion potentials of unlike molecules:

$$\epsilon_{ij} = (1 - k_{ij}) \sqrt{\epsilon_{ii} \epsilon_{jj}} \tag{13}$$

Table 6
CPA binary interaction parameters from literature used in this work.

System	k_{ij}	Association Scheme	Refs.
MEG-H ₂ O	-0.1284	4C	[64]
	-0.1184	4C	
	-0.1460	3C	[56]
	-0.0543	4E	
DEG-H ₂ O	-0.0512	4F	[64]
	-0.1150	4C	
	-0.211	4C	
TEG-H ₂ O	-0.1797	5C	[57]
	-0.1927	4F	
	-0.1478	5F	
	-0.1028	6F	

Table 7
PC-SAFT pure component parameters used in this work. The 4C association scheme was considered for all compounds.

Compound	$\sigma(A)$	$\frac{\epsilon}{k}(K)$	m	$\frac{\epsilon^{AB}}{R}(K)$	κ^{AB}	Refs.
MEG	3.5914	325.23	1.9088	2080.03	0.0235	[67]
DEG	3.6143	310.29	3.0582	2080.03	0.0235	
TEG	4.0186	333.17	2.1809	2080.03	0.0235	
Water	2.6273	180.30	1.5000	1804.22	0.0942	[68]

Table 8
PC-SAFT binary interaction parameters from literature used in this work.

System	k_{ij}	Association Scheme	Refs.
MEG-H ₂ O	-0.046	4C	[67]
DEG-H ₂ O	-0.127		
TEG-H ₂ O	-0.147		

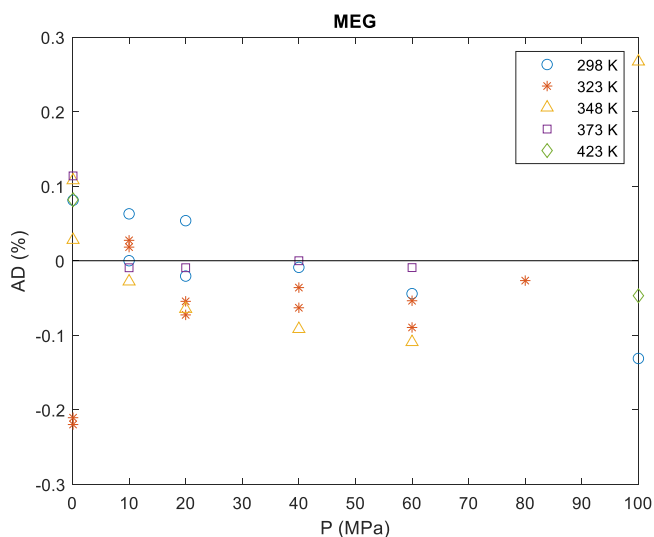


Fig. 2. Percentage average deviations (AD(%)) between density data measured in this work and the ones reported in the literature [21–23,26,27] for monoethylene glycol (MEG) at different temperatures.

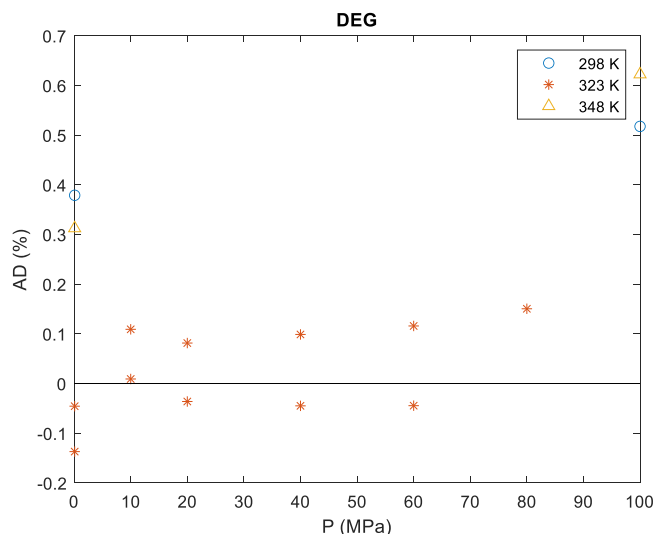


Fig. 3. Percentage average deviations (AD(%)) between density data measured in this work and the ones reported in the literature [26–28] for diethylene glycol (DEG) at different temperatures.

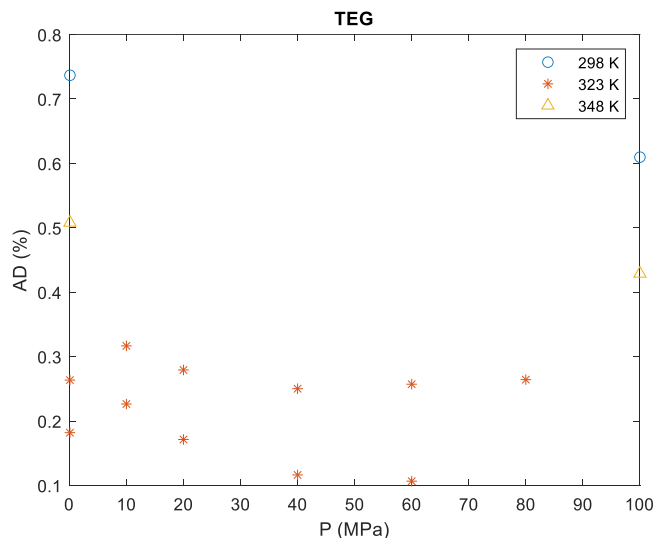


Fig. 4. Percentage average deviations (AD(%)) between density data measured in this work and the ones reported in the literature [26–28] for triethylene glycol (TEG) at different temperatures.

$$\sigma_{ij} = \frac{\sigma_{ii} + \sigma_{jj}}{2} \tag{14}$$

The PC-SAFT pure component parameters and the k_{ij} for the binary systems used in this work are shown in Tables 7 and 8, respectively.

4. Results and discussion

4.1. Literature comparison

Bridgman [14] MEG data presented the highest deviation compared to the measurements reported in this work (−9.8 %), also being in disagreement with the literature data sets (−6.0 %). This is expected due to the indirect technique used in his study. Absolute average relative deviations (AARD) ranging between 0.02 % and 0.09 % were obtained in the comparison between the newly MEG and DEG and the literature data sets, while higher AARD were observed for TEG (0.2 % to 0.3 %). Similarly to Crespo et al. [27] and Yang et al. [22] results, Sagdeev et al.

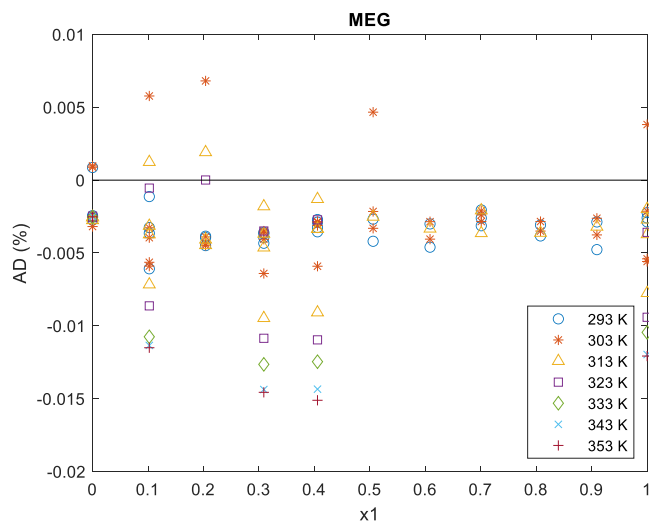


Fig. 5. Percentage average deviations (AD(%)) between density data measured in this work and the ones reported in the literature [30,34–38] for MEG + water at different compositions.

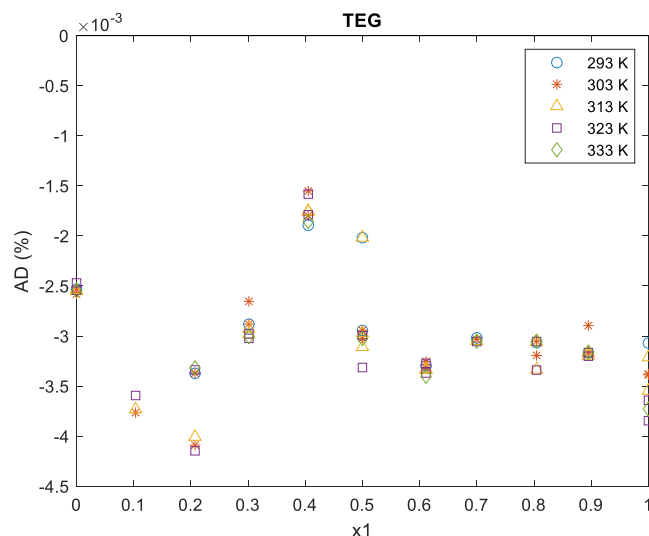


Fig. 7. Percentage average deviations (AD(%)) between density data measured in this work and the ones reported in the literature [33,42,43] for TEG + water at different compositions.

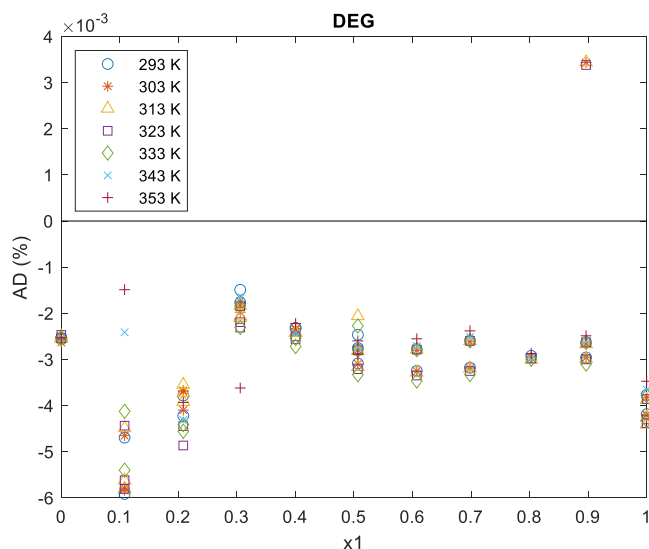


Fig. 6. Percentage average deviations (AD(%)) between density data measured in this work and the ones reported in the literature [33,40,41] for DEG + water at different compositions.

[26] data set presented higher deviations from our measurements in all cases (MEG = 0.1 %, DEG = 0.5 %, and TEG = 0.6 %). Overall, the density data measured in this work present small and no systematic deviations against those available in the literature (Figs. 2–4).

Absolute average relative deviations (AARD) ranging between 0.15 % and 0.35 % were generally found between the newly data and the literature data sets. Yang et al. [36] MEG + water data, however, presented –0.8 % deviation compared to the measurements reported in this work. More significantly, Garcia et al. [39] DEG + water data showed a deviation of –3.4 % from our results. Overall, the density data measured in this work present small and no systematic deviations against those available in the literature (Figs. 5–7).

4.2. Pure component

The experimental data are shown in Table 9. The reported results are, in general, the mean value at a given condition.

The PpT experimental values for each glycol are also illustrated as a

Table 9
Density measurements for Mono-, Di-, and Triethylene glycol between 298.15 K to 423.15 K and up to 140.0 MPa.^a

P (MPa)/ T (K)	Density (g/cm ³)					
	298.15	323.15	348.15	373.15	398.15	423.15
Monoethylene glycol (MEG)						
0.1	1.1081	1.0943	1.0733	1.0530	1.0327	1.0131
10.0	1.1122	1.0962	1.0784	1.0598	1.0383	1.0197
20.0	1.1162	1.1015	1.0834	1.0649	1.0435	1.0259
40.0	1.1244	1.1097	1.0923	1.0744	1.0538	1.0372
60.0	1.1318	1.1177	1.1006	1.0833	1.0635	1.0471
80.0	1.1385	1.1247	1.1082	1.0916	1.0721	1.0569
100.0	1.1451	1.1317	1.1156	1.0991	1.0806	1.0657
120.0	1.1513	1.1383	1.1223	1.1066	1.0884	1.0739
140.0	1.1572	1.1443	1.1289	1.1137	1.0957	1.0817
Diethylene glycol (DEG)						
0.1	1.1098	1.0959	1.0753	1.0547	1.0342	1.0147
10.0	1.1150	1.0991	1.0809	1.0617	1.0401	1.0212
20.0	1.1199	1.1043	1.0861	1.0671	1.0456	1.0279
40.0	1.1282	1.1131	1.0954	1.0772	1.0562	1.0399
60.0	1.1360	1.1212	1.1040	1.0864	1.0665	1.0505
80.0	1.1431	1.1286	1.1120	1.0950	1.0754	1.0604
100.0	1.1497	1.1359	1.1197	1.1029	1.0843	1.0695
120.0	1.1574	1.1428	1.1267	1.1107	1.0923	1.0781
140.0	1.1634	1.1491	1.1335	1.1179	1.1000	1.0862
Triethylene glycol (TEG)						
0.1	1.1115	1.0976	1.0773	1.0564	1.0356	1.0164
10.0	1.1179	1.1020	1.0833	1.0636	1.0419	1.0227
20.0	1.1235	1.1072	1.0887	1.0693	1.0477	1.0298
40.0	1.1320	1.1166	1.0986	1.0799	1.0587	1.0427
60.0	1.1402	1.1248	1.1073	1.0896	1.0696	1.0539
80.0	1.1477	1.1324	1.1159	1.0985	1.0788	1.0640
100.0	1.1543	1.1400	1.1239	1.1067	1.0880	1.0734
120.0	1.1636	1.1473	1.1311	1.1147	1.0962	1.0823
140.0	1.1697	1.1540	1.1381	1.1221	1.1044	1.0907

^a Expanded density uncertainty $U(\rho)$ ($k = 2$) = $7 \cdot 10^{-4}$ g·cm⁻³ for $T < 373.15$ K, $5 \cdot 10^{-3}$ g·cm⁻³ for $T \geq 373.15$ K at 0.1 MPa, and $3 \cdot 10^{-3}$ g·cm⁻³ for $T \geq 373.15$ K and higher pressures, as concluded by Segovia et al. [46]. Standard temperature uncertainty $u(T) = 0.02$ K and standard pressure uncertainty $u(p) = 0.08$ MPa.

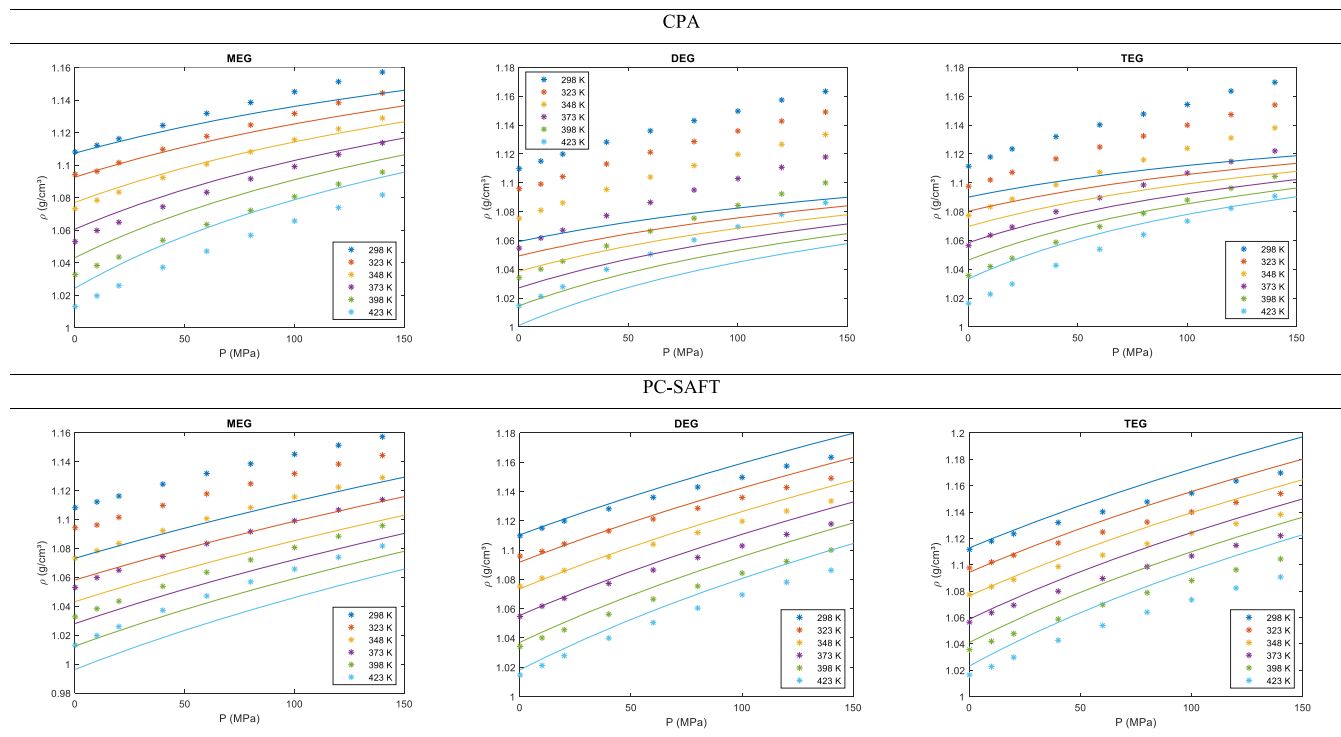


Fig. 8. Glycols PpT data as a function of pressure for the different temperatures studied in this work. Symbols (*) represent experimental data and solid lines thermodynamic modeling. CPA (top row) with MEG-3C, DEG-4C, and TEG-4F association scheme and PC-SAFT (down row) with 4C scheme for all glycols are shown. Parameters are reported in Table 4 and 7.

Table 10

Density Absolute Average Relative Deviation (AARD) for each association scheme considered. The lowest deviation for each compound is indicated in bold letters.

Compound	Association Scheme	Ref.	AARD (%)
CPA			
MEG	4C	[55]	2.0
	4C		1.0
	3C	[56]	0.6
	4E		0.8
DEG	4F		0.8
	4C	[55]	3.7
	4C	[55]	3.7
TEG	5C		1.9
	4F	[57]	1.6
	5F		1.7
	6F		1.8
PC-SAFT			
MEG			2.5
DEG	4C	[68]	0.5
TEG			1.1

Table 11

Modified Tammann-Tait (Eq. (14)) coefficients fitted in this work and AARD (%) between the calculated density values and the newly experimental data.

	MEG	DEG	TEG
A_0 (g.cm ⁻³)	1.3009	1.3746	0.9918
$10^3 \cdot A_1$ (g.cm ⁻³ .K ⁻¹)	-0.56	-0.93	1.35
$10^7 \cdot A_2$ (g.cm ⁻³ .K ⁻²)	-2.80	1.96	-31.50
B_0 (MPa)	767.0420	-108.6154	-77.1471
B_1 (MPa.K ⁻¹)	0.0047	2.2384	1.6942
B_2 (MPa.K ⁻²)	-0.0021	-0.0038	-0.0033
C	0.2048	0.0998	0.0630
AARD (%)	0.13	0.18	0.19

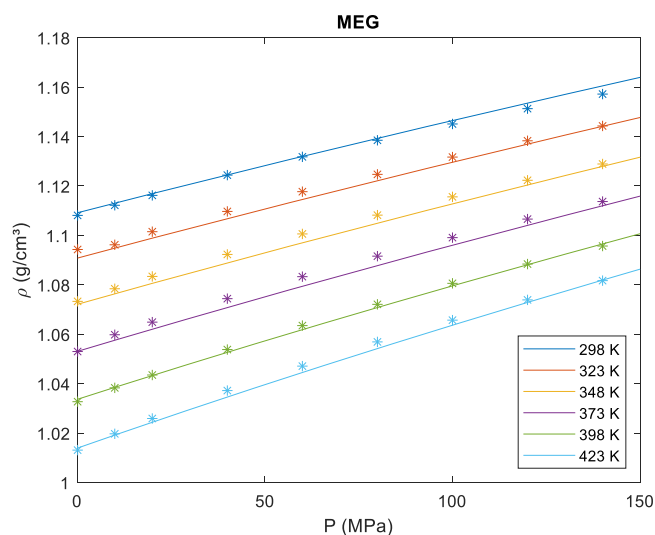


Fig. 9. PpT data for monoethylene glycol as a function of pressure for the different temperatures studied in this work. Symbols (*) represent experimental data and solid lines represent the Tamman-Tait modeling. Parameters are reported in Table 11.

function of pressure for the different temperatures in Fig. 8. The usual trend of density with pressure and temperature can be observed, that is, the density increases with pressure along the isotherms, whereas it decreases with temperature along the isobars for the three glycols studied. The figure also shows the CPA (top row) and the PC-SAFT (bottom row) modeling (lines).

The Absolute Average Relative Deviation (AARD) is given by:

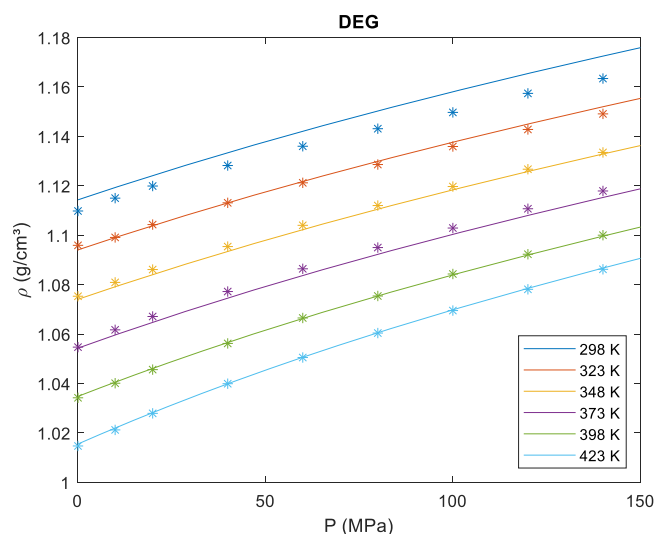


Fig. 10. PpT data for diethylene glycol as a function of pressure for the different temperatures studied in this work. Symbols (*) represent experimental data and solid lines represent the Tamman-Tait modeling. Parameters are reported in Table 11.

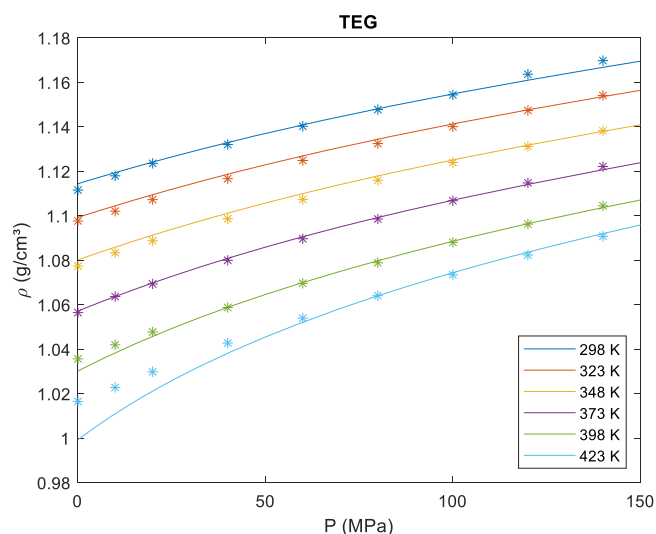


Fig. 11. PpT data for triethylene glycol as a function of pressure for the different temperatures studied in this work. Symbols (*) represent experimental data and solid lines represent the Tamman-Tait modeling. Parameters are reported in Table 11.

$$AARD = \frac{1}{n} \sum_{i=1}^n \left| \frac{\rho_{i,model} - \rho_{i,exp}}{\rho_{i,exp}} \right| \cdot 100(\%) \quad (13)$$

Table 10 presents the AARD obtained for all association schemes studied for each glycol. The lowest deviation for each compound, which was represented in the figures below, is indicated in bold letters.

In the CPA framework, it is noted that the new association schemes proposed for both MEG and TEG improved the model correlation, presenting smaller deviations from the experimental data sets than the original 4C scheme used for glycols. This is expected since Kruger et al. [56] and Qvitsgaard et al. [57] have included Crespo et al. [27] PpT data in their parametrization procedure, while Derawi et al. [55] have used DIPPR 2001 correlations to generate pseudo density data for higher temperatures and pressures. The reparameterization of DEG in a similar way could be an option to optimize its density correlation. Here, it is also interesting to note the poorer results for the heavier glycols. The

Table 12

Isothermal compressibility ($10^4 \cdot \kappa_T (\text{MPa}^{-1})$) and isobaric thermal expansion ($10^4 \cdot \alpha_P (\text{K}^{-1})$), as function of pressure (MPa) and temperature (K) for MEG, DEG, and TEG.

Isothermal Compressibility (MPa^{-1})						
P (MPa)/ T (K)	298.15	323.15	348.15	373.15	398.15	423.15
Monoethylene glycol (MEG)						
0.1	3.53	3.74	4.00	4.32	4.72	5.24
10.0	3.48	3.69	3.94	4.25	4.64	5.14
20.0	3.43	3.63	3.88	4.18	4.55	5.04
40.0	3.35	3.54	3.77	4.05	4.40	4.85
60.0	3.26	3.44	3.66	3.93	4.26	4.68
80.0	3.18	3.36	3.56	3.82	4.13	4.53
100.0	3.11	3.27	3.47	3.71	4.01	4.38
120.0	3.04	3.20	3.38	3.61	3.89	4.24
140.0	2.97	3.12	3.30	3.52	3.79	4.12
Diethylene glycol (DEG)						
0.1	4.59	4.67	4.87	5.21	5.75	6.62
10.0	4.41	4.49	4.67	4.97	5.47	6.25
20.0	4.25	4.31	4.48	4.76	5.21	5.92
40.0	3.95	4.01	4.15	4.39	4.77	5.36
60.0	3.69	3.74	3.87	4.08	4.40	4.90
80.0	3.47	3.51	3.62	3.81	4.09	4.52
100.0	3.27	3.31	3.41	3.57	3.82	4.20
120.0	3.10	3.13	3.22	3.37	3.59	3.92
140.0	2.94	2.97	3.05	3.18	3.38	3.68
Triethylene glycol (TEG)						
0.1	4.67	5.00	5.58	6.58	8.46	1.28
10.0	4.37	4.66	5.16	6.00	7.52	1.08
20.0	4.11	4.36	4.79	5.51	6.77	9.33
40.0	3.67	3.87	4.20	4.75	5.66	7.35
60.0	3.31	3.48	3.75	4.17	4.87	6.08
80.0	3.02	3.16	3.38	3.73	4.28	5.20
100.0	2.78	2.90	3.08	3.37	3.82	4.54
120.0	2.58	2.68	2.84	3.08	3.45	4.04
140.0	2.40	2.49	2.63	2.83	3.15	3.64
Isobaric Expansivity (K^{-1})						
P (MPa)/ T (K)	298.15	323.15	348.15	373.15	398.15	423.15
Monoethylene glycol (MEG)						
0.1	6.51	6.75	7.00	7.26	7.53	7.82
10.0	6.44	6.66	6.89	7.12	7.36	7.59
20.0	6.37	6.57	6.78	6.99	7.18	7.36
40.0	6.23	6.40	6.57	6.73	6.85	6.93
60.0	6.09	6.24	6.37	6.48	6.55	6.54
80.0	5.96	6.09	6.19	6.25	6.26	6.17
100.0	5.84	5.94	6.01	6.03	5.99	5.82
120.0	5.73	5.80	5.84	5.83	5.73	5.49
140.0	5.62	5.67	5.68	5.63	5.48	5.19
Diethylene glycol (DEG)						
0.1	7.31	7.36	7.41	7.45	7.50	7.54
10.0	7.30	7.31	7.31	7.29	7.24	7.13
20.0	7.29	7.26	7.22	7.14	7.01	6.75
40.0	7.28	7.18	7.05	6.88	6.60	6.11
60.0	7.26	7.10	6.91	6.65	6.25	5.57
80.0	7.25	7.04	6.79	6.46	5.95	5.12
100.0	7.24	6.98	6.68	6.28	5.69	4.73
120.0	7.23	6.93	6.59	6.13	5.47	4.39
140.0	7.22	6.89	6.50	5.99	5.26	4.09
Triethylene glycol (TEG)						
0.1	4.73	6.23	7.80	9.46	1.12	1.32
10.0	4.65	6.07	7.53	8.98	1.03	1.08
20.0	4.57	5.93	7.29	8.58	9.55	9.01
40.0	4.44	5.69	6.90	7.94	8.41	6.61
60.0	4.33	5.51	6.60	7.45	7.59	5.02
80.0	4.24	5.35	6.36	7.07	6.96	3.88
100.0	4.17	5.22	6.15	6.76	6.46	3.02
120.0	4.11	5.12	5.98	6.50	6.06	2.33
140.0	4.05	5.02	5.84	6.28	5.72	1.78

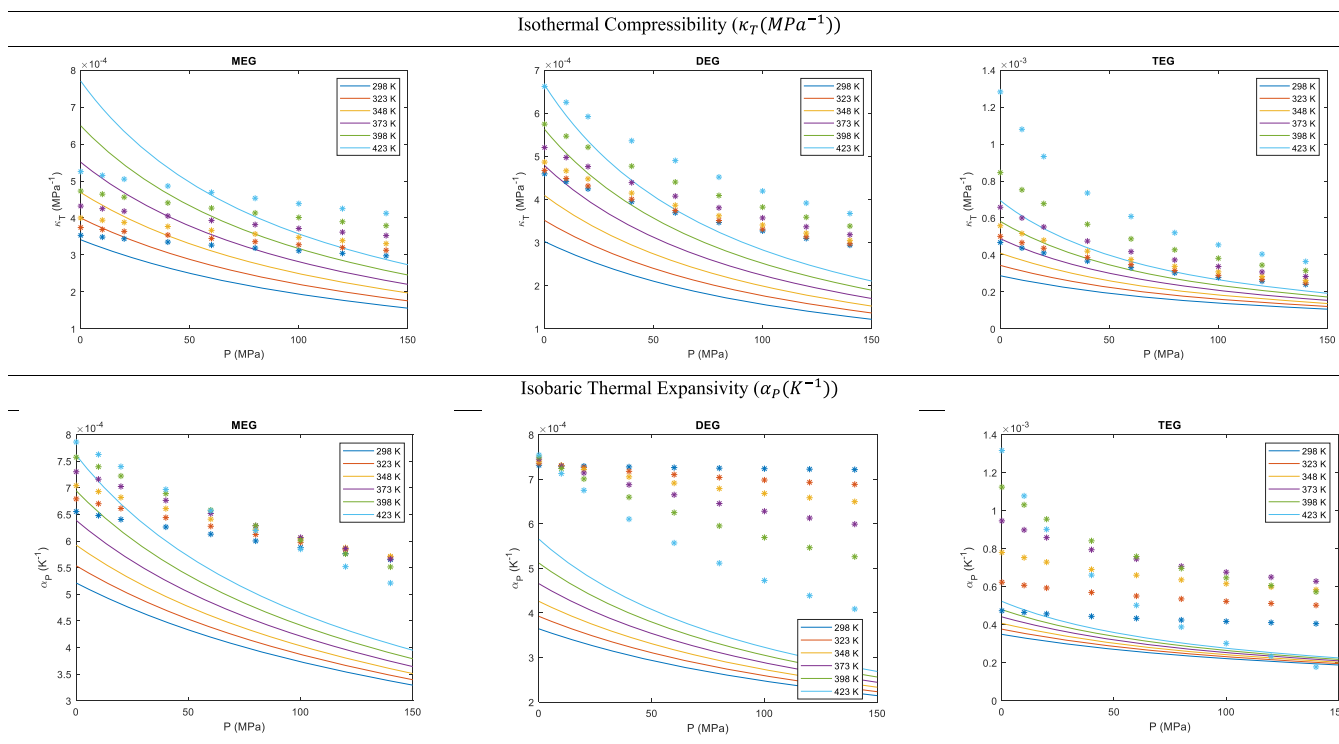


Fig. 12. Glycols isothermal compressibility (top row) and isobaric thermal expansivity (bottom row), as function of pressure (MPa) at different temperatures (K). Symbols (*) represent the derived data obtained with Eqs. (17) and 18 and solid lines represent CPA with MEG-3C, DEG-4C, and TEG-4F association scheme modeling. Parameters are shown in Table 4.

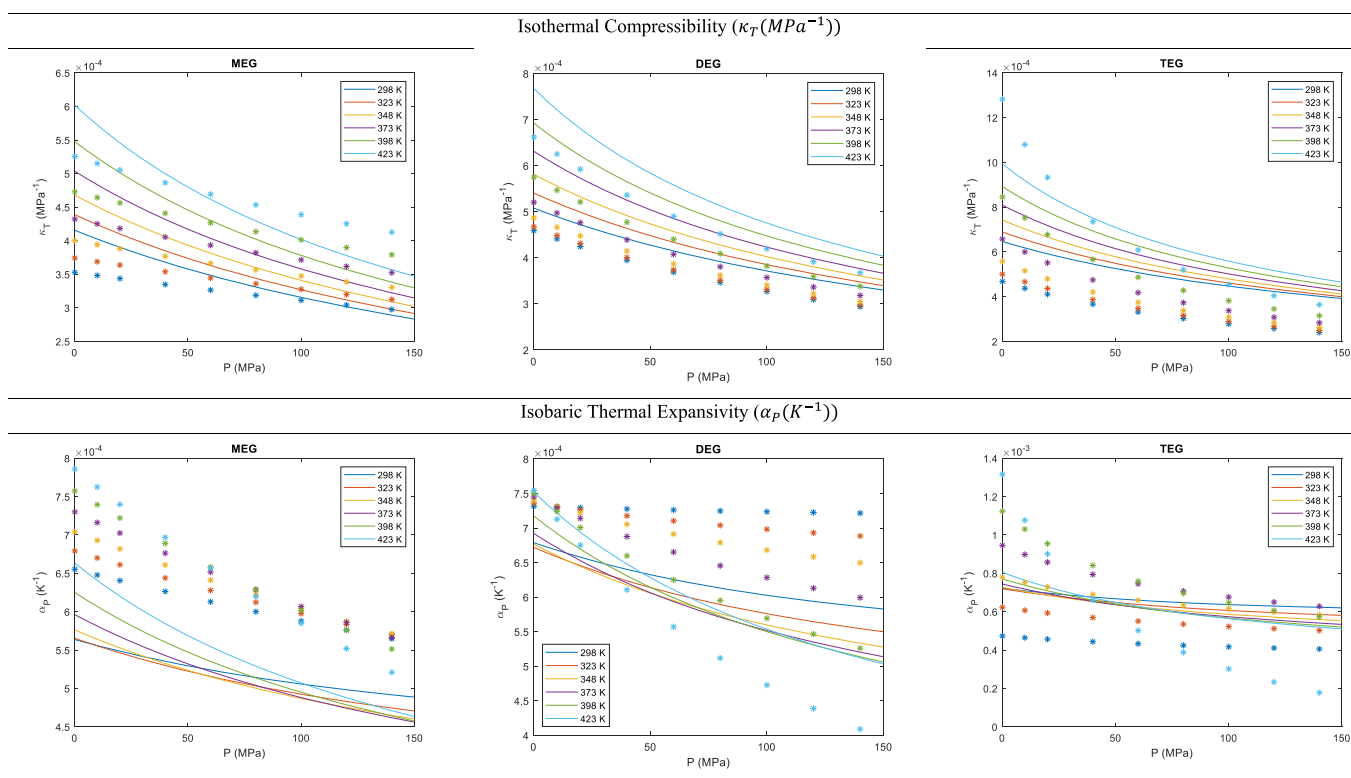


Fig. 13. Glycols isothermal compressibility (top row) and isobaric thermal expansivity (bottom row), as function of pressure (MPa) at different temperatures (K). Symbols (*) represent derived data obtained with Eqs. (17) and 18 and solid lines represent PC-SAFT with 4C association scheme modeling. Parameters are shown in Table 7.

Table 13Binary system density measurements for the mixtures Mono-, Di-, and Triethylene glycol (1) + water (2) between (273.15, 373.15) K at atmospheric pressure.^a

x_1 (mol)/ T (K)	Density (g/cm ³)										
	273.15	283.15	293.15	303.15	313.15	323.15	333.15	343.15	353.15	363.15	373.15
Monoethylene glycol (MEG) (1) + Water (2)											
1.0000	1.13007	1.12316	1.11619	1.10916	1.10208	1.09491	1.08765	1.08028	1.0728	1.06517	1.0574
0.9094	1.12817	1.12125	1.11429	1.10729	1.10021	1.09303	1.08577	1.07838	1.07087	1.06321	1.05539
0.8077	1.12557	1.11864	1.11171	1.10473	1.09766	1.0905	1.08322	1.07582	1.06827	1.06057	1.05269
0.7009	1.12193	1.11513	1.10826	1.10132	1.09427	1.08712	1.07984	1.07242	1.06485	1.0571	1.04916
0.6085	1.11793	1.1112	1.10441	1.09752	1.09052	1.0834	1.07614	1.06872	1.06112	1.05334	1.04536
0.5059	1.11093	1.1045	1.09773	1.09084	1.08382	1.07661	1.06919	1.06132	1.05315	1.04477	1.03632
0.4056	1.10363	1.09736	1.09094	1.08437	1.0776	1.07061	1.06339	1.05624	1.04861	1.04075	1.03186
0.3088	1.09216	1.08670	1.08066	1.07434	1.06792	1.06059	1.05376	1.04673	1.03861	1.03068	1.02283
0.2038	1.07356	1.06942	1.06418	1.05861	1.05268	1.04639	1.03957	1.03173	1.02661	1.01877	1.01186
0.1023	1.04456	1.04208	1.03837	1.03407	1.02922	1.02386	1.01803	1.01175	1.00503	0.99790	0.99038
0.0000	1.00356	1.00223	1.00073	0.99817	0.99473	0.99054	0.98569	0.98024	0.97425	0.96775	0.96043
Diethylene glycol (DEG) (1) + Water (2)											
1.0000	1.13454	1.12838	1.12126	1.11413	1.10697	1.09974	1.09242	1.085	1.07747	1.06979	1.06201
0.8965	1.13376	1.12655	1.11939	1.11223	1.10503	1.09776	1.09049	1.08314	1.07566	1.06802	1.0602
0.8028	1.13352	1.12629	1.11913	1.11196	1.10476	1.09747	1.09019	1.0828	1.07528	1.06761	1.05977
0.6982	1.13202	1.1248	1.11768	1.11048	1.10321	1.09591	1.08856	1.08107	1.07344	1.06561	1.05764
0.6073	1.13063	1.12347	1.11629	1.10907	1.10179	1.09446	1.08706	1.07951	1.07178	1.06388	1.05582
0.5067	1.12805	1.12091	1.11374	1.10653	1.09926	1.09188	1.08446	1.07688	1.06909	1.06109	1.05292
0.4003	1.12336	1.11614	1.10905	1.10188	1.09468	1.0874	1.07999	1.07229	1.06438	1.05622	1.04822
0.3057	1.11535	1.10800	1.10104	1.09426	1.08721	1.07996	1.07255	1.06484	1.05920	1.04872	1.04022
0.2084	1.10335	1.09592	1.08939	1.08270	1.07576	1.06968	1.06237	1.05477	1.04682	1.03875	1.02822
0.1082	1.07735	1.06822	1.06336	1.05797	1.05209	1.04598	1.03926	1.03077	1.02282	1.01569	1.00422
0.0000	1.00356	1.00223	1.00073	0.99817	0.99473	0.99054	0.98569	0.98024	0.97425	0.96775	0.96043
Triethylene glycol (TEG) (1) + Water (2)											
1.0000	1.14184	1.13435	1.12701	1.11958	1.11196	1.10423	1.09645	1.08852	1.08055	1.07251	1.06438
0.8950	1.14144	1.13435	1.12659	1.11883	1.11104	1.10322	1.09535	1.08742	1.07943	1.07136	1.06321
0.8044	1.14084	1.13375	1.12601	1.11826	1.11049	1.10267	1.0948	1.08686	1.07885	1.07075	1.06257
0.6999	1.14052	1.13277	1.12506	1.11736	1.10961	1.1018	1.09392	1.08596	1.07792	1.06979	1.06155
0.6111	1.13952	1.13169	1.12401	1.11632	1.10858	1.10079	1.09292	1.08493	1.07685	1.06867	1.06037
0.4999	1.13777	1.12994	1.12226	1.11456	1.10683	1.09903	1.09114	1.08315	1.07503	1.06678	1.05837
0.4052	1.13347	1.12587	1.11817	1.11042	1.10263	1.09483	1.08697	1.07899	1.07047	1.06167	1.05273
0.3014	1.13037	1.12222	1.11471	1.10713	1.09947	1.09169	1.08378	1.0757	1.06745	1.05904	1.05046
0.2072	1.11958	1.11247	1.10524	1.09787	1.09035	1.08267	1.07483	1.06670	1.05864	1.05017	1.04164
0.1033	1.11758	1.0844	1.07841	1.07212	1.06556	1.05849	1.05138	1.04387	1.03631	1.02827	1.01993
0.0000	1.00356	1.00223	1.00073	0.99817	0.99473	0.99054	0.98569	0.98024	0.97425	0.96775	0.96043

^a Expanded density uncertainty $U(\rho)$ ($k = 2$) = $8 \cdot 10^{-3}$ g·cm⁻³. Standard temperature uncertainty $u(T) = 0.02$ K.

simplified version of PC-SAFT showed overall better results, presenting also some consistency in the correlation trends, systematically under predicting MEG data and overestimating DEG and TEG density for all temperatures in the pressure range evaluated.

The new PpT data were also correlated by means of the following modified Tammann–Tait equation:

$$\rho(T, p) = \frac{\rho(T, 0.1 \text{ MPa})}{1 - C \cdot \ln\left(\frac{B(T) + p}{B(T) + 0.1 \text{ MPa}}\right)} \quad (14)$$

Where $\rho(T, 0.1 \text{ MPa})$ is the density as a function of temperature at a reference pressure, given by the following equation:

$$\rho(T, 0.1 \text{ MPa}) = \sum_{i=0}^2 A_i T^i \quad (15)$$

The $B(T)$ is a temperature-dependent parameter given by:

$$B(T) = \sum_{j=0}^2 B_j T^j \quad (16)$$

Moreover, parameter C is a temperature and pressure independent parameter.

The coefficients A , B , and C were simultaneously regressed minimizing the AARD between experimental and calculated values (Eq. (13)). Table 11 summarizes the fitting parameters obtained for each glycol studied in this work.

The obtained coefficients allow a good description of the experimental PpT data with deviations below 0.2 % as shown in Figs. 9–11.

4.3. Derived properties

The derived properties namely the isothermal compressibility (κ_T) and the isobaric thermal expansion coefficients (α_p) were obtained as derived data from the modified Tammann–Tait coefficient values according to the following equations:

$$\kappa_T(T, p) = \frac{C}{(B(T) + p) \left[1 - C \cdot \ln\left(\frac{B(T) + p}{B(T) + 0.1 \text{ MPa}}\right) \right]} \quad (17)$$

$$\alpha_p(T, p) = \frac{A_1 + 2A_2T}{\rho(T, 0.1 \text{ MPa})} - \frac{C(0.1 \text{ MPa} - p)}{(B(T) + p)(B(T) + 0.1 \text{ MPa})} \left[\frac{B_1 + 2B_2T}{1 - C \cdot \ln\left(\frac{B(T) + p}{B(T) + 0.1 \text{ MPa}}\right)} \right] \quad (18)$$

The calculated values are summarized in Table 12.

The values obtained above are also shown in comparison to CPA (Fig. 12) and PC-SAFT (Fig. 13) modeling. The observed discrepancies between the thermodynamic models (lines) and the derived data (points) can be explained by the indirect method used to calculate these last ones. The isothermal compressibility and the isobaric thermal expansion coefficients data points were calculated by Eqs. (17) and (18), which used the previously adjusted Tammann-Tait coefficients in Table 11. It is noted that with seven coefficients many solutions sets could equally satisfy the Tammann-Tait optimization. In this work, we chose the parameters that resulted in the smallest deviation in relation to the measured density data, which may not be the most suitable set to describe the subsequently derived properties.

The isothermal compressibility (κ_T) of the studied compounds, which reflects the volumetric changes with pressure at a fixed temperature, shows a clear dependency with pressure and temperature, decreasing with increasing pressure and as the temperature decreases as expected. The asymptotic behavior of the isothermal compressibility at high pressure can be explained is that the free space between molecules is more and more reduced, and volume changes are thus more and more limited. Moreover, as the number of ethoxy groups increases the temperature and pressure dependency become less relevant.

The isobaric thermal expansivity (α_p) presents a similar pressure and temperature dependency as the isobaric compressibility. However, it is noted that, as the pressure increases, a cross-over point occurs. This phenomenon, although commonly observed for non-associating com-

pounds, such as n-alkanes [69,70] was firstly reported for glycols by Crespo et al. [27]. These authors explained this behavior as a macroscopic manifestation of the association phenomenon occurring at the molecular level, with the temperature increase leading to hydrogen bonds breaking. This implies decreasing intermolecular interactions that become dominated by dispersive forces such as in for alkanes.

The simplified version of PC-SAFT showed overall qualitative better results, being able to get the cross-over point of isobaric thermal expansivity, while CPA was not able to model this behavior.

4.4. Binary systems

The experimental data for the binary systems glycol (1) + water (2) are presented in Table 13 and they are illustrated as a function of the molar fraction of the glycol (x_1) for the different temperatures in Fig. 14. Table 14 presents the AARD obtained for each of the association schemes studied.

The same usual trend of density with temperature can be observed, that is, the density decreases with temperature for the three systems studied. The simplified version of PC-SAFT showed overall better results, presenting also some consistency in the correlation trends, systematically under predicting MEG data and overestimating DEG and TEG density for all temperatures evaluated. Here, it is also interesting to note the poorer results for the heavier glycols. Once again, the new parameters proposed for both MEG and TEG improved CPA correlation, presenting smaller deviations from the experimental data sets than the original parameters proposed by Derawi et al. [55].

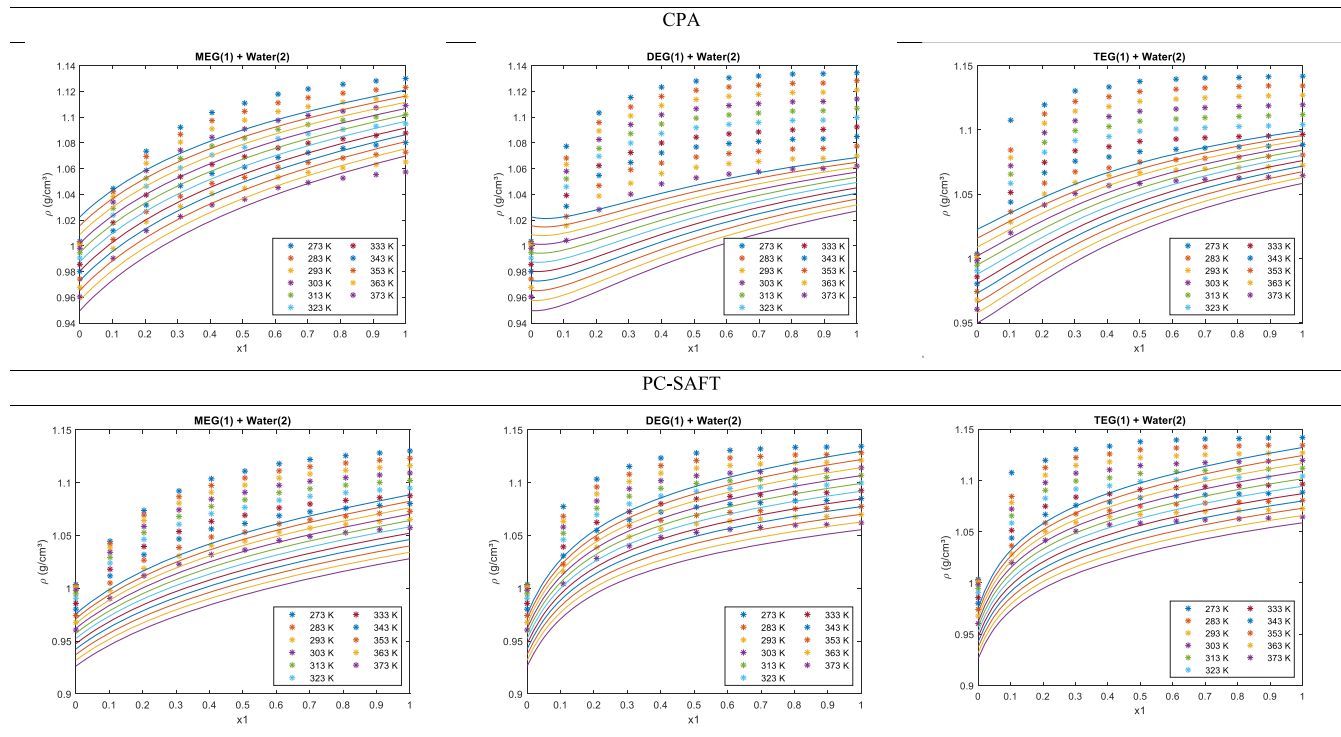


Fig. 14. Binary density data for glycol (1) + water (2) as a function of glycol molar fraction (x_1) for the different temperatures studied in this work. Symbols (*) represent experimental data and solid lines thermodynamic modeling. CPA (top row) with MEG-4C, DEG-4C, and TEG-4F association scheme and PC-SAFT (down row) with 4C scheme for all glycols are shown. Parameters are reported in Table 4, 6, 7, and 8.

Table 14

Binary system density Absolute Average Relative Deviation (AARD) for each association scheme considered in this work. The lowest deviation for each compound is indicated in bold letters.

Compound	Association Scheme	Ref.	AARD (%)
CPA			
MEG	4C	[55]	6.4
	4C		2.5
	3C	[56]	2.7
	4E		3.2
DEG	4F		3.2
	4C	[55]	12.0
	4C	[55]	12.9
TEG	5C		9.1
	4F	[57]	8.6
	5F		8.8
	6F		9.3
PC-SAFT			
MEG			9.9
DEG	4C	[68]	5.6
TEG			6.8

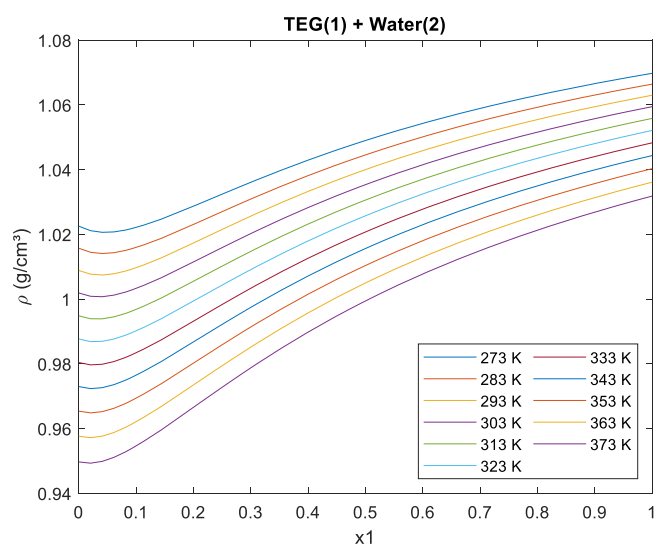


Fig. 15. TEG (1) + water (2) density as a function of glycol molar fraction (x_1) for the different temperatures studied in this work. Solid lines represent CPA modeling with TEG-4C association scheme. Parameters are reported in Table 4 and 6.

The irregular behavior showed by CPA at low glycol concentrations for DEG (1) + water (2) was also observed for the TEG binary system when Derawi et al. [55] 4C association scheme parameters were used for TEG (Fig. 15).

This observation reinforces the statement that DEG reparameterization for different association schemes could result in an optimized density correlation, as the new 4F association scheme for TEG improved the binary density correlation in more than 4 %, showing a better trend also at low glycol concentration.

5. Conclusions

The density of Mono-, Di-, and Triethylene glycol was measured at 6 isotherms (298.15, 323.15, 348.15, 373.15, 398.15, and 423.15 K) and pressures up to 140.0 MPa. Furthermore, the density of the aqueous mixtures for the three glycols have been also measured in the (273.15 to 373.15) K temperature range at atmospheric pressure. Both measurements were made by using a vibrating-tube densimeter. The combined expanded uncertainty ($k = 2$) in the experimental density was estimated to be better than $8 \cdot 10^{-3} \text{ g} \cdot \text{cm}^{-3}$, considering measurement uncertainties relate to temperature, pressure and oscillation period, as well from

instrument calibration and sample impurities. The new values were compared with experimental high-pressure density data reported in the literature and showed low deviations within the stated uncertainty limits.

The modified Tammann-Tait equation was used to correlate the pure component density data, which yields an AARD of less than 0.2 %. The Tait-coefficients were then used to obtain second-order thermodynamic properties, such as isothermal compressibility and isobaric thermal expansion. The CPA and PC-SAFT EoSs were used as molecular modeling tools to describe the reported experimental data with an AARD of less than 4.0 % for the first model and 2.5 % for the last one. It was noted that the correct association schemes to represent glycols is still under discussion in the CPA framework. The simplified version of PC-SAFT showed better results overall, presenting some consistency in the density correlation trends and being able to get the cross-over point of isobaric thermal expansivity, while CPA was not able to model this behavior. For the binary systems, CPA presented AARD less than 12.0 % while PC-SAFT showed less than 10.0 % deviation. Once again, the new parameters proposed for both MEG and TEG improved CPA correlation. Besides the good description of the density's trends, it is noted that the model presents greater difficulty as high molecular weight glycols.

CRedit authorship contribution statement

Julia Trancoso: Conceptualization, Data curation, Software, Visualization, Writing – review & editing. **Georgios M. Kontogeorgis:** Funding acquisition, Supervision. **Xiaodong Liang:** Software, Supervision. **Nicolas von Solms:** Funding acquisition, Supervision.

Declaration of Competing Interest

The authors declare the following financial interests/personal relationships which may be considered as potential competing interests:

Nicolas von Solms reports financial support was provided by Equinor Research centre.

Data availability

Data will be made available on request.

Acknowledgements

The authors gratefully acknowledge the financial and technical support from Equinor A/S (Norway) for this work as part of the research project 'Chemicals for Gas Processing' and the Department of Chemical Engineering, Danmarks Tekniske Universitet (DTU).

References

- [1] S. D.Rebsdats, Mayer, ETHYLENE GLYCOL., Ullmann's Encycl, Ind. Chem. 13 (2012) 531–546, https://doi.org/10.5005/jp/books/11750_18.
- [2] A. Bahadori, H.B. Vuthaluru, S. Mokhtab, Analyzing solubility of acid gas and light alkanes in triethylene glycol, J. Nat. Gas Chem. 17 (2008) 51–58, [https://doi.org/10.1016/S1003-9953\(08\)60025-0](https://doi.org/10.1016/S1003-9953(08)60025-0).
- [3] S. Mokhtab, W.A. Poe, J.Y. Mak, Natural gas dehydration and mercaptans removal, 2019. 10.1016/b978-0-12-815817-3.00009-5.
- [4] L. Saiz, J.A. Padró, E. Guàrdia, Structure of liquid ethylene glycol: a molecular dynamics simulation study with different force fields, J. Chem. Phys. 114 (2001) 3187–3199, <https://doi.org/10.1063/1.1340605>.
- [5] H.Y. Chen, Y.L. Cheng, K. Takahashi, Theoretical calculation of the OH vibrational overtone spectra of 1,5-pentanediol and 1,6-hexanediol, J. Phys. Chem. A 115 (2011) 14315–14324, <https://doi.org/10.1021/jp206202u>.
- [6] Y.P. Chang, T.M. Su, T.W. Li, I. Chao, Intramolecular hydrogen bonding, Gauche interactions, and thermodynamic functions of 1,2-ethanediamine, 1,2-ethanediol, and 2-aminoethanol: a global conformational analysis, J. Phys. Chem. A 101 (1997) 6107–6117, <https://doi.org/10.1021/jp971022j>.
- [7] P. Knauth, R. Sabbah, Energetics of inter- and intramolecular bonds in alkanediols. iv. the thermochemical study of 1,2-alkanediols at 298.15K, Thermochim. Acta 164 (1990) 145–152, [https://doi.org/10.1016/0040-6031\(90\)80431-W](https://doi.org/10.1016/0040-6031(90)80431-W).

- [8] T. Lafitte, M.M. Piñeiro, J.L. Daridon, D. Bessières, A comprehensive description of chemical association effects on second derivative properties of alcohols through a SAFT-VR approach, *J. Phys. Chem. B* 111 (2007) 3447–3461, <https://doi.org/10.1021/jp0682208>.
- [9] M.B. Oliveira, F. Llovel, J.A.P. Coutinho, L.F. Vega, New procedure for enhancing the transferability of statistical associating fluid theory (SAFT) molecular parameters: the role of derivative properties, *Ind. Eng. Chem. Res.* 55 (2016) 10011–10024, <https://doi.org/10.1021/acs.iecr.6b02205>.
- [10] A.J. de Villiers, C.E. Schwarz, A.J. Burger, G.M. Kontogeorgis, Evaluation of the PC-SAFT, SAFT and CPA equations of state in predicting derivative properties of selected non-polar and hydrogen-bonding compounds, *Fluid Phase Equilib.* 338 (2013) 1–15, <https://doi.org/10.1016/j.fluid.2012.09.035>.
- [11] G.M. Kontogeorgis, R. Dohrn, I.G. Economou, J.C. De Hemptinne, A. Kate, S. Kuitunen, M. Mooijer, L.F. Zilnik, V. Vesovic, Industrial requirements for thermodynamic and transport properties: 2020, *Ind. Eng. Chem. Res.* 60 (2021) 4987–5013, <https://doi.org/10.1021/acs.iecr.0c05356>.
- [12] P.J. Carvalho, C.H.G. Fonseca, M.L.C.J. Moita, Á.F.S. Santos, J.A.P. Coutinho, Thermophysical properties of glycols and glymes, *J. Chem. Eng. Data* 60 (2015) 3721–3737, <https://doi.org/10.1021/acs.jced.5b00662>.
- [13] D.I. Sagdeev, M.G. Fomina, G.K. Mukhamedzyanov, I.M. Abdulgatov, Experimental study of the density and viscosity of polyethylene glycols and their mixtures at temperatures from 293K to 473K and at atmospheric pressure, *J. Chem. Thermodyn.* 43 (2011) 1824–1843, <https://doi.org/10.1016/j.jct.2011.06.013>.
- [14] P.W. Bridgman, *Volume-Temperature-Pressure Relations for Several Non-Volatile Liquids*, *Proc. Am. Acad. Arts Sci.* 67 (1932) 1–27.
- [15] C.F. Wong, W. Hayduk, Molecular diffusivities for propene in 1-butanol, chlorobenzene, ethylene glycol, and n-octane at elevated pressures, 1990.
- [16] Y. Miyamoto, M. Takemoto, M. Hosokawa, Y. Uosaki, T. Moriyoshi, Compressions of (water + a C3 alkane) and (water + an alkane-1,2-diol) at the temperature 298.15K and pressures up to 200MPa, *J. Chem. Thermodyn.* 22 (1990) 1007–1014, [https://doi.org/10.1016/0021-9614\(90\)90190-2](https://doi.org/10.1016/0021-9614(90)90190-2).
- [17] B. Guignon, C. Aparicio, P.D. Sanz, Volumetric properties of pressure-transmitting fluids up to 350 MPa: water, ethanol, ethylene glycol, propylene glycol, castor oil, silicon oil, and some of their binary mixture, *J. Chem. Eng. Data* 55 (2010) 3017–3023, <https://doi.org/10.1021/je9010568>.
- [18] G.I. Egorov, D.M. Makarov, Compressibility of ethylene glycol-dimethyl sulfoxide mixtures over the pressure range 0.1–100MPa at 308.15K, *Russ. J. Phys. Chem. A* 85 (2011) 171–178, <https://doi.org/10.1134/S0036024411020105>.
- [19] G.I. Egorov, D.M. Makarov, A.M. Kolker, Liquid phase PVTx properties of binary mixtures of (water+ethylene glycol) in the range from 278.15 to 323.15K and from 0.1 to 100MPa. I. Experimental results, partial and excess thermodynamics properties, *Fluid Phase Equilib.* 344 (2013) 125–138, <https://doi.org/10.1016/j.fluid.2013.01.025>.
- [20] A.M.K. Gennadiy I. Egorov, Dmitriy M. Makarov, Densities and volumetric properties of ethylene glycol + dimethylsulfoxide mixtures at temperatures of (278.15 to 323.15) K and pressures of (0.1 to 100) MPa, *J. Chem. Eng. Data* 55 (2010) 3481–3488, <https://doi.org/10.1021/acs.jced.7b00750>.
- [21] M. Atilhan, S. Aparicio, PpT measurements and derived properties of liquid 1,2-alkanediols, *J. Chem. Thermodyn.* 57 (2013) 137–144, <https://doi.org/10.1016/j.jct.2012.08.014>.
- [22] X. Yang, C.C. Sampson, O. Frotscher, M. Richter, Measurement and correlation of the (p , ρ , T) behaviour of liquid ethylene glycol at temperatures from (283.3 to 393.1) K and pressures up to 100.1MPa, *J. Chem. Thermodyn.* 144 (2020), 106054, <https://doi.org/10.1016/j.jct.2020.106054>.
- [23] M.M. Zarić, M. Vraneš, S. Bikić, A. Tot, S. Papović, T.T. Borović, M.L. Kijevčanin, I. R. Radović, Thermodynamic properties of caffeine in ethylene glycol at high pressures and high temperatures, *J. Chem. Eng. Data* 67 (2022) 3351–3363, <https://doi.org/10.1021/acs.jced.2c00401>.
- [24] W.V. Steele, R.D. Chirico, A.B. Cowell, S.E. Knipmeyer, A. Nguyen, Thermodynamic properties and ideal-gas enthalpies of formation for methyl benzoate, ethyl benzoate, (R)-(+)-limonene, tert-amyl methyl ether, trans-crotonaldehyde, and diethylene glycol, *J. Chem. Eng. Data* 47 (2002) 667–688, <https://doi.org/10.1021/je0100847>.
- [25] W.V. Steele, R.D. Chirico, S.E. Knipmeyer, A. Nguyen, Measurements of vapor pressure, heat capacity, and density along the saturation line for ϵ -caprolactam, pyrazine, 1,2-propanediol, triethylene glycol, phenyl acetylene, and diphenyl acetylene, *J. Chem. Eng. Data* 47 (2002) 689–699, <https://doi.org/10.1021/je010085z>.
- [26] D.I. Sagdeev, M.G. Fomina, G.K. Mukhamedzyanov, I.M. Abdulgatov, Experimental study of the density and viscosity of polyethylene glycols and their mixtures at temperatures from 293K to 465K and at high pressures up to 245MPa, *Fluid Phase Equilib.* 315 (2012) 64–76, <https://doi.org/10.1016/j.fluid.2011.11.022>.
- [27] E.A. Crespo, J.M.L. Costa, Z.B.M.A. Hanafiah, K.A. Kurnia, M.B. Oliveira, F. Llovel, L.F. Vega, P.J. Carvalho, J.A.P. Coutinho, New measurements and modeling of high pressure thermodynamic properties of glycols, *Fluid Phase Equilib.* 436 (2017) 113–123, <https://doi.org/10.1016/j.fluid.2017.01.003>.
- [28] M.F.V. Pereira, H.M.N.T. Avelino, F.J.P. Caetano, J.M.N.A. Fareira, Viscosity of liquid diethylene, triethylene and tetraethylene glycols at moderately high pressures using a vibrating wire instrument, *Fluid Phase Equilib.* 480 (2019) 87–97, <https://doi.org/10.1016/j.fluid.2018.09.026>.
- [29] W. Hayduk, V.K. Malik, Density, viscosity, and carbon dioxide solubility and diffusivity in aqueous ethylene glycol solutions, *J. Chem. Eng. Data* 16 (1971) 143–146, <https://doi.org/10.1021/je60049a005>.
- [30] M. Dizechi, E. Marschall, Viscosity of Some Binary and Ternary Liquid Mixtures, *J. Chem. Eng. Data* 27 (1982) 358–363, <https://doi.org/10.1021/je00029a039>.
- [31] V.K. Reddy, K.S. Reddy, A. Krishnaiah, Excess volumes, speeds of sound, and viscosities for mixtures of 1,2-ethanediol and alkoxy alcohols with water at 308.15K, *J. Chem. Eng. Data* 39 (1994) 615–617, <https://doi.org/10.1021/je00015a051>.
- [32] T.M. Aminabhavi, B. Gopalakrishna, Density, Viscosity, Refractive Index, and Speed of Sound in Binary, (1996) 632–641.
- [33] T. Sun, A.S. Teja, Density, viscosity and thermal conductivity of aqueous solutions of propylene glycol, dipropylene glycol, and tripropylene glycol between 290K and 460K, *J. Chem. Eng. Data* 49 (2004) 1311–1317, <https://doi.org/10.1021/je049960h>.
- [34] H. Lee, W.H. Hong, H. Kim, Excess volumes of binary and ternary mixtures of water, methanol, and ethylene glycol, *J. Chem. Eng. Data* 35 (1990) 371–374, <https://doi.org/10.1021/je00061a040>.
- [35] N.G. Tsierekos, I.E. Molinou, Thermodynamic properties of water + ethylene glycol at 283.15, 293.15, 303.15, and 313.15K, *J. Chem. Eng. Data* 43 (1998) 989–993, <https://doi.org/10.1021/je9800914>.
- [36] C. Yang, P. Ma, F. Jing, D. Tang, Excess molar volumes, viscosities, and heat capacities for the mixtures of ethylene glycol + water from 273.15K to 353.15K, *J. Chem. Eng. Data* 48 (2003) 836–840, <https://doi.org/10.1021/je020140j>.
- [37] J. Zhang, P. Zhang, K. Ma, F. Han, G. Chen, X. Wei, Hydrogen bonding interactions between ethylene glycol and water: density, excess molar volume, and spectral study, *Sci. China Ser. B Chem.* 51 (2008) 420–426, <https://doi.org/10.1007/s11426-008-0045-0>.
- [38] M. Moosavi, A.A. Rostami, Densities, viscosities, refractive indices, and excess properties of aqueous 1,2-ethanediol, 1,3-propanediol, 1,4-butanediol, and 1,5-pentanediol binary mixtures, *J. Chem. Eng. Data* 62 (2017) 156–168, <https://doi.org/10.1021/acs.jced.6b00526>.
- [39] J.M. Bernal-García, A. Guzmán-López, A. Cabrales-Torres, V. Rico-Ramírez, G. A. Iglesias-Silva, Supplementary densities and viscosities of aqueous solutions of diethylene glycol from (283.15 to 353.15) K, *J. Chem. Eng. Data* 53 (2008) 1028–1031, <https://doi.org/10.1021/je700672f>.
- [40] S.K. Begum, R.J. Clarke, M.S. Ahmed, S. Begum, M.A. Saleh, Densities, viscosities, and surface tensions of the system water + diethylene glycol, *J. Chem. Eng. Data* 56 (2011) 303–306, <https://doi.org/10.1021/je1009976>.
- [41] K. Klimaszewski, E. Stronka-Lewkowska, K. Sowiłoda, A. Bald, Acoustic and volumetric studies on water + diethylene glycol mixtures in a wide temperature range. Comparison with mixtures of water with tri- and tetraethylene glycol, *J. Mol. Liq.* 215 (2016) 520–533, <https://doi.org/10.1016/j.molliq.2016.01.037>.
- [42] S.K. Begum, R.J. Clarke, M.S. Ahmed, S. Begum, M.A. Saleh, Volumetric, viscosimetric and surface properties of aqueous solutions of triethylene glycol, tetraethylene glycol, and tetraethylene glycol dimethyl ether, *J. Mol. Liq.* 177 (2013) 11–18, <https://doi.org/10.1016/j.molliq.2012.09.015>.
- [43] K. Klimaszewski, E. Stronka-Lewkowska, K. Abramczyk, A. Bald, Acoustic and volumetric studies on (triethylene glycol + water) mixtures in a wide temperature range, *J. Chem. Thermodyn.* 89 (2015) 212–222, <https://doi.org/10.1016/j.jct.2015.05.024>.
- [44] M. Morénas, G. Douhéret, Thermodynamic behaviour of some glycol-water mixtures. Excess and partial volumes, *Thermochim. Acta* 25 (1978) 217–224, [https://doi.org/10.1016/0040-6031\(78\)80059-6](https://doi.org/10.1016/0040-6031(78)80059-6).
- [45] E.A. Müller, P. Rasmussen, Densities and excess volumes in aqueous poly(ethylene glycol) solutions, *J. Chem. Eng. Data* 36 (1991) 214–217, <https://doi.org/10.1021/je00002a019>.
- [46] J.J. Segovia, O. Fandiño, E.R. López, L. Lugo, M. Carmen Martín, J. Fernández, Automated densimetric system: measurements and uncertainties for compressed fluids, *J. Chem. Thermodyn.* 41 (2009) 632–638, <https://doi.org/10.1016/j.jct.2008.12.020>.
- [47] M.J.P. Comuñas, J. Bazile, A. Baylaucq, C. Boned, M.J.P. Comuñas, *, †, ‡ Jean-Patrick Bazile, † Antoine Baylaucq, † and Christian Boned †, *Engineering*. (2008) 986–994.
- [48] T. Regueira, W. Yan, E.H. Stenby, Densities of the binary systems n-hexane + n-decane and n-hexane + n-hexadecane up to 60MPa and 463K, *J. Chem. Eng. Data* 60 (2015) 3631–3645, <https://doi.org/10.1021/acs.jced.5b00613>.
- [49] T. Regueira, G. Pantelide, W. Yan, E.H. Stenby, Density and phase equilibrium of the binary system methane + n-decane under high temperatures and pressures, *Fluid Phase Equilib.* 428 (2016) 48–61, <https://doi.org/10.1016/j.fluid.2016.08.004>.
- [50] T. Regueira, M.L. Glykioti, E.H. Stenby, W. Yan, Density and compressibility of multicomponent n-alkane mixtures up to 463K and 140MPa, *J. Chem. Eng. Data* 63 (2018) 1072–1080, <https://doi.org/10.1021/acs.jced.7b00803>.
- [51] G.M. Kontogeorgis, E.C. Voutsas, I.V. Yakoumis, D.P. Tassios, An equation of state for associating fluids, *Ind. Eng. Chem. Res.* 35 (1996) 4310–4318, <https://doi.org/10.1021/ie9600203>.
- [52] M.L. Michelsen, E.M. Hendriks, Physical properties from association models, *Fluid Phase Equilib.* 180 (2001) 165–174, [https://doi.org/10.1016/S0378-3812\(01\)00344-2](https://doi.org/10.1016/S0378-3812(01)00344-2).
- [53] W.G. Chapman, K.E. Gubbins, G. Jackson, M. Radosz, SAFT: equation-of-state solution model for associating fluids, *Fluid Phase Equilib.* 52 (1989) 31–38, [https://doi.org/10.1016/0378-3812\(89\)80308-5](https://doi.org/10.1016/0378-3812(89)80308-5).
- [54] G.M. Kontogeorgis, I.V. Yakoumis, H. Meijer, E. Hendriks, T. Moorwood, Multicomponent phase equilibrium calculations for water–methanol–alkane mixtures, *Fluid Phase Equilib.* 158–160 (1999) 201–209, [https://doi.org/10.1016/S0378-3812\(99\)00060-6](https://doi.org/10.1016/S0378-3812(99)00060-6).
- [55] S.O. Derawi, M.L. Michelsen, G.M. Kontogeorgis, E.H. Stenby, Application of the CPA equation of state to glycol/hydrocarbons liquid-liquid equilibria, *Fluid Phase Equilib.* 209 (2003) 163–184, [https://doi.org/10.1016/S0378-3812\(03\)00056-6](https://doi.org/10.1016/S0378-3812(03)00056-6).

- [56] F. Kruger, G.M. Kontogeorgis, N. von Solms, New association schemes for mono-ethylene glycol: cubic-Plus-Association parameterization and uncertainty analysis, *Fluid Phase Equilib.* 458 (2018) 211–233, <https://doi.org/10.1016/j.fluid.2017.11.026>.
- [57] D. Qvistgaard, F. Kruger, X. Liang, G.M. Kontogeorgis, N. von Solms, New association schemes for tri-ethylene glycol: cubic-Plus-Association parameterization and uncertainty analysis, *Fluid Phase Equilib.* 551 (2022), 113254, <https://doi.org/10.1016/j.fluid.2021.113254>.
- [58] G.M. Kontogeorgis, I.V. Yakoumis, H. Meijer, E. Hendriks, T. Moorwood, Multicomponent phase equilibrium calculations for water-methanol-alkane mixtures, *Fluid Phase Equilib.* 158–160 (1999) 201–209, [https://doi.org/10.1016/S0378-3812\(99\)00060-6](https://doi.org/10.1016/S0378-3812(99)00060-6).
- [59] S.H. Huang, M. Radosz, Equation of state for small, large, polydisperse, and associating molecules: extension to fluid mixtures, *Ind. Eng. Chem. Res.* 30 (1991) 1994–2005, <https://doi.org/10.1021/ie00056a050>.
- [60] G.K. Folas, Modeling of complex mixtures containing hydrogen bonding molecules, *Chem. Eng.* (2006).
- [61] F.J. Kruger, M.V. Danielsen, G.M. Kontogeorgis, E. Solbraa, N. Von Solms, Ternary vapor-liquid equilibrium measurements and modeling of ethylene glycol (1) + water (2) + methane (3) systems at 6 and 12.5MPa, *J. Chem. Eng. Data* 63 (2018) 1789–1796, <https://doi.org/10.1021/acs.jced.8b00115>.
- [62] F.J. Kruger, G.M. Kontogeorgis, E. Solbraa, N. Von Solms, Multicomponent vapor-liquid equilibrium measurement and modeling of ethylene glycol, water, and natural gas mixtures at 6 and 12.5MPa, *J. Chem. Eng. Data* 63 (2018) 3628–3639, <https://doi.org/10.1021/acs.jced.8b00495>.
- [63] G.K. Folas, O.J. Berg, E. Solbraa, A.O. Fredheim, G.M. Kontogeorgis, M. L. Michelsen, E.H. Stenby, High-pressure vapor-liquid equilibria of systems containing ethylene glycol, water and methane. Experimental measurements and modeling, *Fluid Phase Equilib.* 251 (2007) 52–58, <https://doi.org/10.1016/j.fluid.2006.11.001>.
- [64] O. Chiavone-Filho, P. Proust, P. Rasmussen, Vapor-Liquid Equilibria for Glycol Ether + Water Systems, *J. Chem. Eng. Data* 38 (1993) 128–131, <https://doi.org/10.1021/je00009a031>.
- [65] J. Gross, G. Sadowski, Reply to comment on “perturbed-chain SAFT: an equation of state based on a perturbation theory for chain molecules, *Ind. Eng. Chem. Res.* 58 (2019) 5744–5745, <https://doi.org/10.1021/acs.iecr.9b01515>.
- [66] N. Von Solms, M.L. Michelsen, G.M. Kontogeorgis, Computational and physical performance of a modified PC-SAFT equation of state for highly asymmetric and associating mixtures, *Ind. Eng. Chem. Res.* 42 (2003) 1098–1105, <https://doi.org/10.1021/ie020753p>.
- [67] A. Grenner, G.M. Kontogeorgis, N. von Solms, M.L. Michelsen, Application of PC-SAFT to glycol containing systems - PC-SAFT towards a predictive approach, *Fluid Phase Equilib.* 261 (2007) 248–257, <https://doi.org/10.1016/j.fluid.2007.04.025>.
- [68] A. Grenner, J. Schmelzer, N. Von Solms, G.M. Kontogeorgis, Comparison of two association models (Elliott-Suresh-Donohue and simplified PC-SAFT) for complex phase equilibria of hydrocarbon-water and amine-containing mixtures, *Ind. Eng. Chem. Res.* 45 (2006) 8170–8179, <https://doi.org/10.1021/ie0605332>.
- [69] P. Navia, J. Trancoso, L. Román, Isobaric thermal expansivity behaviour against temperature and pressure of associating fluids, *J. Chem. Thermodyn.* 42 (2010) 23–27, <https://doi.org/10.1016/j.jct.2009.07.002>.
- [70] Y. Miyake, A. Baylaucq, F. Plantier, D. Bessières, H. Ushiki, C. Boned, High-pressure (up to 140MPa) density and derivative properties of some (pentyl-, hexyl-, and heptyl-) amines between (293.15 and 353.15) K, *J. Chem. Thermodyn.* 40 (2008) 836–845, <https://doi.org/10.1016/j.jct.2008.01.006>.